

Spin correlations in polarizations of P-wave charmonia χ_{cJ} and impact on J/ψ polarization

Hua-Sheng Shao^(a), Kuang-Ta Chao^(a,b)

(a) Department of Physics and State Key Laboratory of Nuclear Physics and Technology, Peking University, Beijing 100871, China

(b) Center for High Energy Physics, Peking University, Beijing 100871, China

Based on a general form of the effective vertex functions for the decays of P-wave charmonia χ_{cJ} , compact formulas for the angular distributions of the J/ψ in the $\chi_{cJ} \rightarrow J/\psi\gamma$ decay and the muon in the subsequently cascade decay $\chi_{cJ} \rightarrow J/\psi\gamma \rightarrow \mu^+\mu^-\gamma$ are derived. While the former are the same as those obtained in a different approach by using the angular momentum relation, the latter ones are new. Similar to the J/ψ case, the χ_{cJ} polarization observables can be expressed in terms of rational functions of the yields spin density matrix elements of χ_{cJ} . A reweighting method is proposed to determine the production spin density matrix elements of the χ_{c2} . Some generalized rotation-invariant relations for arbitrary integer-spin particles are also derived. Special cases are applied to the polarizations of χ_{c1} and χ_{c2} . In particular, we discuss the possible impact of χ_{cJ} and ψ' feed-down on the prompt J/ψ polarization. As a phenomenological illustration, we present the angular distributions in terms of the spin density matrix elements of χ_{c1} and χ_{c2} production in four different frames at the Large Hadron Collider.

PACS numbers: 13.60.Le, 13.88.+e, 14.40.Pq

I. INTRODUCTION

The polarization of heavy quarkonium in hadroproduction e.g. at the Tevatron and the LHC has been a long-standing issue in heavy quarkonium physics[1]. Non-relativistic QCD (NRQCD)[2], a rigorous effective field theory that characterizes the nonrelativistic feature of heavy quarkonium, gives the description that a $Q\bar{Q}$ pair may be formed in a color-octet (CO) state during the hard reaction at short-distances before its hadronization into a color-singlet (CS) physical quarkonium by radiating soft gluons. Hence, J/ψ , a $c\bar{c}$ bound state with quantum number $J^{PC} = 1^{--}$, is produced dominantly by gluon fragmentation into $c\bar{c}[^3S_1^{[8]}]$ first and it then evolves into $^3S_1^{[1]}$ in the high transverse momentum region[3]. The gluon fragmentation mechanism guarantees that the J/ψ is produced in the transverse polarization in its helicity frame (HX) when its p_T is sufficient large, considering that spin flipping is order of v^2 suppressed according to the power counting rule in NRQCD, where v is the relative velocity between c and \bar{c} . However, the data measured by the CDF[4, 5] Collaboration at the Tevatron indicate that the J/ψ is mainly unpolarized and even slightly longitudinal polarized at large p_T , say, up to 20 GeV. The situation for $\psi(2S)$ is similar to J/ψ . This is the polarization puzzle of heavy quarkonium production.

The importance of charmonium polarization is also related to the efficiency uncertainty that the detector acceptance for lepton pairs from the J/ψ (or other heavy quarkonium) decay strongly depends on its polarization[6], thus the lack of a consistent description of the polarization in the simulation of the quarkonium may result in one of the largest systematic errors that may affect the measurement precision. Besides, polar-

ization observables can provide more information on the production and decay mechanisms than the unpolarized observables. Given these considerations, the polarization issue becomes one of the important topics in quarkonium physics for theorists and experimentalists.

Experimentally, the analysis of direct J/ψ production at hadron colliders is lacking. The measured prompt J/ψ data include direct production and feed-down contributions from the χ_c and ψ' by the radiative decays $\chi_c \rightarrow J/\psi\gamma$, $\psi' \rightarrow J/\psi\gamma$, and $\psi' \rightarrow \chi_c\gamma \rightarrow J/\psi\gamma\gamma$. Therefore, in order to compare the theoretical results with experiment data, one should also investigate the χ_c and ψ' yields besides the J/ψ . Moreover, the χ_c meson has its own phenomenological interest. The ratio of differential cross sections of χ_{c1} to χ_{c2} inclusive production at the Tevatron has been measured by the CDF Collaboration[7]. Their results show that the ratio disagrees with the spin symmetry perspective from the leading-order (LO) computation. After including the next-to-leading (NLO) QCD radiative correction[8], the asymptotic behavior of $\frac{d\sigma}{dp_T^2}$ changes from p_T^{-6} at LO to p_T^{-4} at NLO for the $^3P_J^{[8]}$ channel and hence becomes comparable with the contribution of $^3S_1^{[8]}$ at large p_T . The result provides an opportunity to resolve the contradiction between the experiment and the theoretical prediction. Recently, the LHCb Collaboration[9] shows that their result of $\frac{d\sigma_{\chi_{c2}}}{d\sigma_{\chi_{c1}}}$ stays within the error bar of the NLO NRQCD prediction. Surely, as in the J/ψ case, the investigation of polarization of χ_c will also be very helpful in understanding the production mechanism in QCD.

We now briefly review the recent progress of heavy quarkonium in hadroproduction. In Ref.[10], it is found that the NLO corrections for the yields of hard part of

J/ψ in the $^3S_1^{[1]}$ channel can be as large as two orders of magnitude as compared with LO at large p_T , while NLO corrections for the CO S-wave are small[11]. For the P-wave, the NLO corrections for $^3P_J^{[1]}$ channel [8] and $^3P_J^{[8]}$ channel[12–14] are found to be very large but negative. As for polarization, the NLO correction for the CS channel[15] of the direct J/ψ alters from transverse polarization in HX at LO to longitudinal polarization at NLO, which can be understood in collinear factorization up to the NLO power in $\frac{m^2}{p_T^2}$ [16]. However, even after including NNLO* [17], in which only tree-level diagrams at α_s^5 are considered and infrared cutoffs $s_{ij,min}$ are imposed to avoid soft and collinear divergences, theoretical predictions of CS contributions to the production rates and polarizations are still in disagreement with the CDF data[4, 5]. Recently, two groups[18, 19] have presented their NLO results for the J/ψ direct production at hadron colliders, but drawn very different conclusions due to different treatments for the fit procedure of available data, and extracted different CO long-distance matrix elements (LDMEs). The former[18] uses a global fit, while the latter[19] just concentrates on hadroproduction. The LDMEs in Ref.[19] are more satisfactory for the hadron collider data both in yields and polarization of the J/ψ . Especially, the predictions of yields at the LHC are in good agreement with data[20, 21] up to 70 GeV, and the polarizations of $jpsi$ at the Tevatron and the LHC are predicted to be mainly unpolarized[19].

The study of angular distributions of J/ψ from the χ_c decay has been done in Ref.[23] and the authors have also calculated the spin density matrix elements (SDMEs) of χ_{c1} and χ_{c2} at the Tevatron Run I. The angular distribution formulas have also been derived in Ref.[24]. In the present paper, we re-derive the same expressions for the J/ψ angular distribution in a different way, and we further consider the subsequent decay of the J/ψ into a muon pair. Measurement of the muon angular distribution in the rest frame of J/ψ is an additional informative result for this process. For the presentation of our results with phenomenological application, we have computed the inclusive χ_{c1} and χ_{c2} production at the LHC with the center-of-mass energy 8 TeV.

The organization of the paper is as follows. In section II, we introduce the basic kinematics and conventions used in the paper. In the next three sections, we derive the angular distributions of the J/ψ and the μ^+ from the decays of χ_{c1} and χ_{c2} . In section VI, a re-weighting method is proposed to extract all of the SDMEs of the χ_{c2} . In section VII, we generalize the rotation-invariant relations from the vector boson to arbitrary integer-spin particles, and we show that these observables are frame-independent. In section VIII, we demonstrate the uncertainty of J/ψ polarization from the feed-down of χ_c and ψ' decays. In section IX, we present the numerical results and discuss the corresponding phenomenology. Finally, the conclusion is drawn in the last section. The general expressions of the angular distributions for the spin-1 and

spin-2 bosons are listed in the appendices.

II. KINEMATICS AND CONVENTIONS

In this section, we introduce the conventions and kinematics for our derivations performed in the following sections. We consider the decay process of $\chi_{cJ} \rightarrow J/\psi\gamma$ and the subsequent one $J/\psi \rightarrow \mu^+\mu^-$. Experimentally, one is able to reconstruct J/ψ 's momentum from its decay products $\mu^+\mu^-$, which can be identified efficiently at detectors. One can always choose an arbitrary axis as the spin-quantization axis \vec{s} in its rest frame. Generally, the polarization vectors for a massive spin-1 particle are

$$\begin{aligned}\epsilon_0^\mu &= (|\vec{k}|, E \sin \theta \cos \phi, E \sin \theta \sin \phi, E \cos \theta)/m, \\ \epsilon_\pm^\mu &= \frac{e^{\mp i\gamma}}{\sqrt{2}}(0, \mp \cos \theta \cos \phi + i \sin \phi, \\ &\quad \mp \cos \theta \sin \phi - i \cos \theta, \pm \sin \theta),\end{aligned}\quad (1)$$

where θ, ϕ are the polar and azimuthal angles of \vec{s} and the symbol γ can be chosen as an arbitrary real number. We set $\gamma = -\phi$ here. For a spin-2 tensor particle, its spin wave functions can be constructed from the spin-1 polarization 4-vectors as

$$\epsilon_\lambda^{\mu\nu} = \sum_{\lambda_1, \lambda_2=-1}^1 \langle 1, \lambda_1; 1, \lambda_2 | 2, \lambda \rangle \epsilon_{\lambda_1}^\mu \epsilon_{\lambda_2}^\nu, \quad (2)$$

where $\langle 1, \lambda_1; 1, \lambda_2 | 2, \lambda \rangle$ are the Clebsch-Gordan coefficients. Thus we have identities $p_\mu \epsilon_\lambda^\mu = p_\mu \epsilon_\lambda^{\mu\nu} = p_\nu \epsilon_\lambda^{\mu\nu} = (\epsilon_\lambda)_\mu^\mu = 0$ and $\epsilon_\lambda^{\mu\nu} = \epsilon_\lambda^{\nu\mu}$.

In $\chi_{cJ} \rightarrow J/\psi\gamma \rightarrow \mu^+\mu^-\gamma$, one can work out the angular distributions of J/ψ in a form of the χ_{cJ} production SDMEs $\rho_{\lambda\lambda'}$ and decay SDMEs $D_{\lambda\lambda'}$

$$\mathcal{W}(\theta, \phi) = \sum_{\lambda, \lambda'=-J}^J \rho_{\lambda\lambda'} D_{\lambda\lambda'}(\theta, \phi), \quad (3)$$

where θ, ϕ are the polar and azimuthal angles of the J/ψ or the μ^+ in the χ_{cJ} rest frame. Here $\rho_{\lambda\lambda'}$ and $D_{\lambda\lambda'}$ represent the production and decay amplitudes of the χ_{cJ} with spin λ multiplied by the corresponding complex conjugate amplitudes with spin λ' .

Several polarization frame definitions have been used in the literature to fully describe the polarization of heavy quarkonium. They are the so-called HX (recoil or s-channel helicity frame), the Collins-Soper frame, the Gottfried-Jackson frame and the target frame[25]. In HX, \vec{s} is chosen as the flight direction of the quarkonium, while in the Collins-Soper frame \vec{s} bisects the angle between \vec{p}_1 and $-\vec{p}_2$ in the rest frame of the quarkonium, where \vec{p}_1 and \vec{p}_2 denote the momenta of the two initial state colliding particles in the quarkonium rest frame. In the Gottfried-Jackson frame $\vec{s} = \frac{\vec{p}_1}{|\vec{p}_1|}$ and in the target frame $\vec{s} = -\frac{\vec{p}_2}{|\vec{p}_2|}$. Here the quarkonium means χ_c in the case of hadroproduction process $pp(\bar{p}) \rightarrow \chi_c + X$.

III. ANGULAR DISTRIBUTIONS IN $\chi_{c1} \rightarrow J/\psi\gamma$

The general vertex function for a vector or axial vector decays into two vectors can be expressed as

$$\begin{aligned} \mathcal{M}(V_0 \rightarrow V_1 V_2) = & a \epsilon_{V_0} \cdot \epsilon_{V_1}^* \epsilon_{V_2}^* \cdot (-p_{V_0} - p_{V_1}) \\ & + b \epsilon_{V_0} \cdot \epsilon_{V_2}^* \epsilon_{V_1}^* \cdot (p_{V_0} + p_{V_2}) \\ & + c \epsilon_{V_1}^* \cdot \epsilon_{V_2}^* \epsilon_{V_0} \cdot (p_{V_1} - p_{V_2}) \\ & + d \epsilon_{V_0} \cdot (p_{V_1} - p_{V_2}) \epsilon_{V_1}^* \cdot (p_{V_0} + p_{V_2}) \\ & \epsilon_{V_2}^* \cdot (p_{V_0} + p_{V_1}) + f i \varepsilon_{\epsilon_{V_0} \epsilon_{V_1}^* \epsilon_{V_2}^* p_{V_0}} \\ & + g \epsilon_{V_1}^* \cdot (p_{V_0} + p_{V_2}) i \varepsilon_{\epsilon_{V_0} \epsilon_{V_2}^* p_{V_0} p_{V_2}} \\ & + h \epsilon_{V_2}^* \cdot (p_{V_0} + p_{V_1}) i \varepsilon_{\epsilon_{V_0} \epsilon_{V_1}^* p_{V_0} p_{V_1}}, \end{aligned} \quad (4)$$

where

$$p_{V_0} = p_{V_1} + p_{V_2}, \varepsilon_{\mu\nu\rho k} \equiv \varepsilon_{\mu\nu\rho\sigma} k^\sigma.$$

Specifically, in the case of $\chi_{c1}(1^{++}) \rightarrow J/\psi(1^{--})\gamma(1^{--})$, the a, b, c, d terms and the h term can be dropped, because of parity conservation in QED and no longitudinal polarization for the photon. If we just consider the electric dipole (E1) transition, which is the dominant contribution according to the velocity scaling rule in NRQCD, the g term can also be negligible. Therefore, we calculate the helicity amplitudes $\mathcal{M}_{\lambda_{\chi_{c1}} \lambda_{J/\psi} \lambda_\gamma}$ for $\chi_{c1} \rightarrow J/\psi\gamma$ (with "f" suppressed) as

$$\begin{aligned} \mathcal{M}_{+++} &= \mathcal{M}_{---}^* = \frac{m_{\chi_{c1}} e^{-i\phi} \sin \theta}{\sqrt{2}}, \\ \mathcal{M}_{+--} &= \mathcal{M}_{-++}^* = -\frac{m_{\chi_{c1}} e^{3i\phi} \sin \theta}{\sqrt{2}}, \\ \mathcal{M}_{+0+} &= -\mathcal{M}_{-0-} = -\frac{(m_{\chi_{c1}}^2 + m_{J/\psi}^2) \sin^2 \frac{\theta}{2}}{2m_{J/\psi}}, \\ \mathcal{M}_{+0-} &= -\mathcal{M}_{-0+}^* = \frac{(m_{\chi_{c1}}^2 + m_{J/\psi}^2) e^{2i\phi} \cos^2 \frac{\theta}{2}}{2m_{J/\psi}}, \\ \mathcal{M}_{0++} &= -\mathcal{M}_{0--}^* = -m_{\chi_{c1}} e^{-2i\phi} \cos \theta, \\ \mathcal{M}_{00+} &= \mathcal{M}_{00-}^* = \frac{(m_{\chi_{c1}}^2 + m_{J/\psi}^2) e^{-i\phi} \sin \theta}{2\sqrt{2}m_{J/\psi}}, \end{aligned} \quad (5)$$

where a common factor $m_{\chi_{c1}}^2 - m_{J/\psi}^2$ has also been suppressed. The decay SDMEs are obtained by $D_{\lambda\lambda'} = \sum_{\lambda_{J/\psi}, \lambda_\gamma} \mathcal{M}_{\lambda\lambda_{J/\psi}\lambda_\gamma} \mathcal{M}_{\lambda'\lambda_{J/\psi}\lambda_\gamma}^*$. Using these ingredients, we can work out the general form of angular distribution of J/ψ from the χ_{c1} decay

$$\begin{aligned} \mathcal{W}^{\chi_{c1} \rightarrow J/\psi\gamma}(\theta, \phi) &= \frac{N_{\chi_{c1} \rightarrow J/\psi\gamma}}{3 + \lambda_\theta} (1 + \lambda_\theta \cos^2 \theta \\ &+ \lambda_\phi \sin^2 \theta \cos 2\phi + \lambda_{\theta\phi} \sin 2\theta \cos \phi \\ &+ \lambda_\phi^\perp \sin^2 \theta \sin 2\phi + \lambda_{\theta\phi}^\perp \sin 2\theta \sin \phi), \end{aligned} \quad (6)$$

with

$$\begin{aligned} \lambda_\theta &= \frac{3\rho_{0,0} - N_{\chi_{c1}}}{3N_{\chi_{c1}} - \rho_{0,0}}, \lambda_\phi = -\frac{2\Re\rho_{1,-1}}{3N_{\chi_{c1}} - \rho_{0,0}}, \\ \lambda_{\theta\phi} &= -\frac{\sqrt{2}(\Re\rho_{1,0} - \Re\rho_{-1,0})}{3N_{\chi_{c1}} - \rho_{0,0}}, \\ \lambda_\phi^\perp &= \frac{2\Im\rho_{1,-1}}{3N_{\chi_{c1}} - \rho_{0,0}}, \lambda_{\theta\phi}^\perp = \frac{\sqrt{2}(\Im\rho_{1,0} + \Im\rho_{-1,0})}{3N_{\chi_{c1}} - \rho_{0,0}}, \end{aligned} \quad (7)$$

where $\rho_{i,j}$ are SDMEs for the χ_{c1} yields and $N_{\chi_{c1}} = \rho_{1,1} + \rho_{0,0} + \rho_{-1,-1}$.

IV. ANGULAR DISTRIBUTIONS IN $\chi_{c2} \rightarrow J/\psi\gamma$

Similarly, for the χ_{c2} we can write down the general vertex function for a spin-2 tensor particle T_2 decays into two vectors

$$\begin{aligned} \mathcal{M}(T_2 \rightarrow V_1 V_2) = & a \epsilon_{V_2}^* \cdot \epsilon_{T_2} \cdot \epsilon_{V_1}^* \\ & + b (p_{V_1} - p_{V_2}) \cdot \epsilon_{T_2} \cdot \epsilon_{V_1}^* \epsilon_{V_2}^* \cdot (-p_{T_2} - p_{V_1}) \\ & + c (p_{V_1} - p_{V_2}) \cdot \epsilon_{T_2} \cdot \epsilon_{V_2}^* \epsilon_{V_1}^* \cdot (p_{T_2} + p_{V_2}) \\ & + d (p_{V_1} - p_{V_2}) \cdot \epsilon_{T_2} \cdot (p_{V_1} - p_{V_2}) \epsilon_{V_1}^* \cdot \epsilon_{V_2}^* \\ & + f (p_{V_1} - p_{V_2}) \cdot \epsilon_{T_2} \cdot (p_{V_1} - p_{V_2}) \\ & \epsilon_{V_1}^* \cdot (p_{T_2} + p_{V_2}) \epsilon_{V_2}^* \cdot (p_{T_2} + p_{V_1}) \\ & + \text{Levi-Civita terms}, \end{aligned} \quad (8)$$

where $p_{T_2} = p_{V_1} + p_{V_2}$. Due to parity conservation, we drop the Levi-Civita terms in $\chi_{c2}(2^{++}) \rightarrow J/\psi(1^{--})\gamma(1^{--})$. b, c, d, f terms can also be ignored in consideration of the fact that we only include the leading order contribution, i.e. the E1 transition, and these terms are suppressed by $(m_{\chi_{c2}}^2 - m_{J/\psi}^2)^2$ as compared to the a term, and some terms should vanish when the photon is transversely polarized. Thus, the helicity amplitudes

$\mathcal{M}_{\lambda_{\chi_{c2}} \lambda_{J/\psi} \lambda_\gamma}$ for $\chi_{c2} \rightarrow J/\psi \gamma$ become

$$\begin{aligned}
\mathcal{M}_{2++} &= \mathcal{M}_{2--} = \frac{\sin^2 \theta}{4}, \\
\mathcal{M}_{2+-} &= \mathcal{M}_{2-+}^* = e^{2i\phi} \cos^4 \frac{\theta}{2}, \\
\mathcal{M}_{2--} &= \mathcal{M}_{2++}^* = \frac{e^{4i\phi} \sin^2 \theta}{4}, \\
\mathcal{M}_{2-+} &= \mathcal{M}_{2+-}^* = e^{2i\phi} \sin^4 \frac{\theta}{2}, \\
\mathcal{M}_{20+} &= -\mathcal{M}_{20-}^* = -\frac{m_{\chi_{c2}}^2 + m_{J/\psi}^2}{\sqrt{2} m_{\chi_{c2}} m_{J/\psi}} e^{i\phi} \sin^3 \frac{\theta}{2} \cos \frac{\theta}{2}, \\
\mathcal{M}_{20-} &= -\mathcal{M}_{20+}^* = -\frac{m_{\chi_{c2}}^2 + m_{J/\psi}^2}{\sqrt{2} m_{\chi_{c2}} m_{J/\psi}} e^{3i\phi} \cos^3 \frac{\theta}{2} \sin \frac{\theta}{2}, \\
\mathcal{M}_{1++} &= -\mathcal{M}_{1--}^* = -\frac{e^{-i\phi} \sin 2\theta}{4}, \\
\mathcal{M}_{1+-} &= -\mathcal{M}_{1-+}^* = 2e^{i\phi} \cos^3 \frac{\theta}{2} \sin \frac{\theta}{2}, \\
\mathcal{M}_{1--} &= -\mathcal{M}_{1++}^* = -\frac{e^{3i\phi} \sin 2\theta}{4}, \\
\mathcal{M}_{1-+} &= -\mathcal{M}_{1+-}^* = -2e^{i\phi} \sin^3 \frac{\theta}{2} \cos \frac{\theta}{2}, \\
\mathcal{M}_{10+} &= \mathcal{M}_{10-} = \frac{m_{\chi_{c2}}^2 + m_{J/\psi}^2}{2\sqrt{2} m_{\chi_{c2}} m_{J/\psi}} \sin^2 \frac{\theta}{2} (1 + 2 \cos \theta), \\
\mathcal{M}_{10-} &= \mathcal{M}_{10+}^* = \frac{m_{\chi_{c2}}^2 + m_{J/\psi}^2}{2\sqrt{2} m_{\chi_{c2}} m_{J/\psi}} e^{2i\phi} \cos^2 \frac{\theta}{2} (2 \cos \theta - 1), \\
\mathcal{M}_{0++} &= \mathcal{M}_{0--}^* = \frac{e^{-2i\phi} (1 + 3 \cos 2\theta)}{4\sqrt{6}}, \\
\mathcal{M}_{0+-} &= \mathcal{M}_{0-+} = \frac{3 \sin^2 \theta}{2\sqrt{6}}, \\
\mathcal{M}_{00+} &= -\mathcal{M}_{00-}^* = -\frac{\sqrt{3} (m_{\chi_{c2}}^2 + m_{J/\psi}^2)}{8 m_{\chi_{c2}} m_{J/\psi}} e^{-i\phi} \sin 2\theta. \quad (9)
\end{aligned}$$

The angular distribution of J/ψ from the χ_{c2} decay is

$$\begin{aligned}
\mathcal{W}^{\chi_{c2} \rightarrow J/\psi \gamma}(\theta, \phi) &= \frac{N_{\chi_{c2} \rightarrow J/\psi \gamma}}{3 + \lambda_\theta} (1 + \lambda_\theta \cos^2 \theta) \quad (10) \\
&+ \lambda_\phi \sin^2 \theta \cos 2\phi + \lambda_{\theta\phi} \sin 2\theta \cos \phi \\
&+ \lambda_\phi^\perp \sin^2 \theta \sin 2\phi + \lambda_{\theta\phi}^\perp \sin 2\theta \sin \phi
\end{aligned}$$

with

$$\begin{aligned}
\lambda_\theta &= \frac{6N_{\chi_{c2}} - 9(\rho_{1,1} + \rho_{-1,-1}) - 12\rho_{0,0}}{6N_{\chi_{c2}} + 3(\rho_{1,1} + \rho_{-1,-1}) + 4\rho_{0,0}}, \\
\lambda_\phi &= \frac{2\sqrt{6}(\Re\rho_{2,0} + \Re\rho_{-2,0}) + 6\Re\rho_{1,-1}}{6N_{\chi_{c2}} + 3(\rho_{1,1} + \rho_{-1,-1}) + 4\rho_{0,0}}, \\
\lambda_{\theta\phi} &= \frac{6(\Re\rho_{2,1} - \Re\rho_{-2,-1}) + \sqrt{6}(\Re\rho_{1,0} - \Re\rho_{-1,0})}{6N_{\chi_{c2}} + 3(\rho_{1,1} + \rho_{-1,-1}) + 4\rho_{0,0}}, \\
\lambda_\phi^\perp &= -\frac{2\sqrt{6}(\Im\rho_{2,0} - \Im\rho_{-2,0}) + 6\Im\rho_{1,-1}}{6N_{\chi_{c2}} + 3(\rho_{1,1} + \rho_{-1,-1}) + 4\rho_{0,0}}, \\
\lambda_{\theta\phi}^\perp &= -\frac{6(\Im\rho_{2,1} + \Im\rho_{-2,-1}) + \sqrt{6}(\Im\rho_{1,0} + \Im\rho_{-1,0})}{6N_{\chi_{c2}} + 3(\rho_{1,1} + \rho_{-1,-1}) + 4\rho_{0,0}}, \\
N_{\chi_{c2}} &= \rho_{2,2} + \rho_{1,1} + \rho_{0,0} + \rho_{-1,-1} + \rho_{-2,-2}. \quad (11)
\end{aligned}$$

If one wants to include not only E1, but also magnetic quadrupole (M2) and electric octupole (E3) contributions, the angular distribution becomes much more complicated. Nevertheless, one can calculate these contributions easily by just keeping the coefficients in the χ_{c1} and χ_{c2} vertex functions independent and following the above procedures. After normalization, there are one and two remaining coefficients for χ_{c1} and χ_{c2} respectively that should be extracted from experimental data. We have presented them in the appendices. However, one should be reminded that when the coefficients of M2 and E3 contributions are not very small, changes of angular distributions due to the higher-order multipole terms may also be significant[24] and then one should include these contributions in the calculations. The unknown higher-order multipole coefficients need to be extracted from experiment. However, present measurements of these higher-order multipole amplitudes are still not sufficiently precise and even inconsistent[26–29], and including the M2 and E3 transitions also makes the physical analysis more complicated but still does not change the underlying physics. Hence, only E1 transition is considered throughout the main context, and we put the formula including the higher-order multipole effects in the appendices, which can be used in practical calculations.

Our results Eq.(7) and Eq.(11) are exactly the same as those given in Refs.[23, 24]. Actually, our derivations, which are based on the general effective decay vertex functions, are equivalent to those by using the angular momentum analysis as done in Refs.[23, 24], since the effective amplitudes written by us are also originated from general considerations of spins of involved particles.

V. SPIN CORRELATIONS IN

$$\chi_{cJ} \rightarrow J/\psi \gamma \rightarrow \mu^+ \mu^- \gamma$$

We are now in a position to investigate the μ^+ angular distributions from the cascade decay $\chi_{cJ} \rightarrow J/\psi \gamma \rightarrow \mu^+ \mu^- \gamma$.

We start from a general formalism to study it. For the polarization of χ_{cJ} , we suppose its quantization axis

as \vec{s}_1^z , while that for J/ψ is denoted as \vec{s}_2^z . Then, the general form for the angular distribution of the μ^+ is

$$\begin{aligned} & \mathcal{W}^{\chi_{cJ} \rightarrow J/\psi \gamma \rightarrow \mu^+ \mu^- \gamma}(\theta', \phi') \\ &= \int d^2\Omega[\theta, \phi] \rho_{J_z, J_z'}^{\chi_{cJ}} \mathcal{M}_{J_z s_z \lambda_\gamma}^{\chi_{cJ} \rightarrow J/\psi \gamma}(\theta, \phi) \mathcal{M}_{s_z \lambda_{\mu^+} \lambda_{\mu^-}}^{J/\psi \rightarrow \mu^+ \mu^-}(\theta', \phi') \\ & \quad \left(\mathcal{M}_{J_z' s_z' \lambda_\gamma}^{\chi_{cJ} \rightarrow J/\psi \gamma}(\theta, \phi) \mathcal{M}_{s_z' \lambda_{\mu^+} \lambda_{\mu^-}}^{J/\psi \rightarrow \mu^+ \mu^-}(\theta', \phi') \right)^*, \end{aligned} \quad (12)$$

where $\rho_{J_z, J_z'}^{\chi_{cJ}}$ are production SDMEs of the χ_{cJ} , $\mathcal{M}_{J_z s_z \lambda_\gamma}^{\chi_{cJ} \rightarrow J/\psi \gamma}$, $\mathcal{M}_{s_z \lambda_{\mu^+} \lambda_{\mu^-}}^{J/\psi \rightarrow \mu^+ \mu^-}$ are the decay amplitudes¹ with the lower indices representing their spin or helicity and θ, ϕ denotes as the J/ψ 's polar and azimuthal angles respect to \vec{s}_1^z in the rest frame of the χ_{cJ} and θ', ϕ' denotes as the μ^+ 's polar and azimuthal angles respect to \vec{s}_2^z in the rest frame of the J/ψ . Conventionally, the indices that appear twice imply a summation here, i.e. $J_z, J_z' = \pm J, \pm(J-1), \dots, 0$, $s_z, s_z' = \pm 1, 0$ and $\lambda_\gamma, \lambda_{\mu^+}, \lambda_{\mu^-} = \pm$. We emphasize that J_z, J_z' are respected to \vec{s}_1^z , while s_z, s_z' to \vec{s}_2^z . Again, one can also use the general angular momentum relations with proper rotations to the specific reference axis to calculate the angular distribution function $\mathcal{W}^{\chi_{cJ} \rightarrow J/\psi \gamma \rightarrow \mu^+ \mu^- \gamma}(\theta', \phi')$. Nevertheless, they are equivalent for reasons that have been given in the previous section.

Now, we consider the first scenario in which \vec{s}_2^z is defined as the flight direction of the J/ψ in the rest frame of χ_{cJ} . With the same parametrization as in Eqs.(6,10), there are five observables in terms of the χ_{cJ} SDMEs $\rho_{J_z, J_z'}^{\chi_{cJ}}$

$$\begin{aligned} \lambda_{\theta'}^{\chi_{c1}} &= -\frac{1}{3}, \lambda_{\phi'}^{\chi_{c1}} = \lambda_{\phi'}^{\perp \chi_{c1}} = 0, \\ \lambda_{\theta' \phi'}^{\chi_{c1}} &= \frac{\sqrt{2}(\Re(\rho_{1,0}^{\chi_{c1}}) - \Re(\rho_{-1,0}^{\chi_{c1}}))}{12N_{\chi_{c1}}}, \\ \lambda_{\theta' \phi'}^{\perp \chi_{c1}} &= -\frac{\sqrt{2}(\Im(\rho_{1,0}^{\chi_{c1}}) + \Im(\rho_{-1,0}^{\chi_{c1}}))}{12N_{\chi_{c1}}}, \\ \lambda_{\theta'}^{\chi_{c2}} &= \frac{1}{13}, \\ \lambda_{\phi'}^{\chi_{c2}} &= \frac{7\sqrt{6}(\Re(\rho_{0,2}^{\chi_{c2}}) + \Re(\rho_{0,-2}^{\chi_{c2}})) + 12\Re(\rho_{1,-1}^{\chi_{c2}})}{78N_{\chi_{c2}}}, \\ \lambda_{\theta' \phi'}^{\chi_{c2}} &= \frac{\sqrt{6}(\Re(\rho_{-1,0}^{\chi_{c2}}) - \Re(\rho_{1,0}^{\chi_{c2}})) + 24(\Re(\rho_{-2,-1}^{\chi_{c2}}) - \Re(\rho_{2,1}^{\chi_{c2}}))}{156N_{\chi_{c2}}}, \\ \lambda_{\theta' \phi'}^{\perp \chi_{c2}} &= \frac{7\sqrt{6}(\Im(\rho_{0,2}^{\chi_{c2}}) - \Im(\rho_{0,-2}^{\chi_{c2}})) - 12\Im(\rho_{1,-1}^{\chi_{c2}})}{78N_{\chi_{c2}}}, \\ \lambda_{\theta' \phi'}^{\perp \chi_{c2}} &= \frac{\sqrt{6}(\Im(\rho_{-1,0}^{\chi_{c2}}) + \Im(\rho_{1,0}^{\chi_{c2}})) + 24(\Im(\rho_{-2,-1}^{\chi_{c2}}) + \Im(\rho_{2,1}^{\chi_{c2}}))}{156N_{\chi_{c2}}}, \end{aligned} \quad (13)$$

with $N_{\chi_{cJ}} = \sum_{\lambda=-J}^J \rho_{\lambda\lambda}^{\chi_{cJ}}$. In the language of angular momentum theory, the spin correlations between $\rho_{J_z, J_z'}^{\chi_{cJ}}$

with quantization axis \vec{s}_1^z and $\rho_{s_z, s_z'}^{\chi_{cJ} \rightarrow J/\psi \gamma}$ with quantization axis \vec{s}_2^z can be written as

$$\begin{aligned} \rho_{s_z, s_z'}^{\chi_{cJ} \rightarrow J/\psi \gamma} &= \frac{3}{8\pi} \int d\Omega[\theta, \phi] \rho_{J_z, J_z'}^{\chi_{cJ}} \mathcal{D}_{J_z, J_{1z}}^{J*} \mathcal{D}_{J_z', J_{2z}}^J \\ & \langle 1, \lambda_\gamma; 1, s_z | J, J_{1z} \rangle \langle J, J_{2z} | 1, \lambda_\gamma; 1, s_z' \rangle \text{Br}(\chi_{cJ} \rightarrow J/\psi \gamma), \end{aligned} \quad (14)$$

where the summation is also implicitly understood with $\lambda_\gamma = \pm$, $J_z, J_z', J_{1z}, J_{2z} = \pm J, \dots, 0$, and $\text{Br}(\chi_{cJ} \rightarrow J/\psi \gamma)$ represents the branching ratio of χ_{cJ} decays into a J/ψ plus a photon, and $\mathcal{D}_{J_z, J_z'}^J \equiv \mathcal{D}_{J_z, J_z'}^J(-\phi, \theta, \phi) = e^{i\phi(J_z - J_z')} d_{J_z, J_z'}^J(\theta)$, with $d_{J_z, J_z'}^J(\theta)$ are the well-known Wigner d -function

$$\begin{aligned} d_{J_z, J_z'}^J(\theta) &= \sum_{k=\max(0, J_z' - J_z)}^{\min(J + J_z', J - J_z)} (-1)^{k - J_z' + J_z} \\ & \times \frac{\sqrt{(J + J_z')!(J - J_z')!(J + J_z)!(J - J_z)!}}{(J + J_z' - k)!k!(J - J_z - k)!(k - J_z' + J_z)!} \\ & \times \left(\cos \frac{\theta}{2} \right)^{2J - 2k + J_z' - J_z} \left(\sin \frac{\theta}{2} \right)^{2k - J_z' + J_z}. \end{aligned} \quad (15)$$

One can easily verify that after substituting $\rho_{s_z, s_z'}^{\chi_{cJ} \rightarrow J/\psi \gamma}$ calculated from the above equation into the well-known angular distribution of the muon from $J/\psi \rightarrow \mu^+ \mu^-$

$$\begin{aligned} \lambda_{\theta'}^{J/\psi} &= \frac{N_{J/\psi} - 3\rho_{0,0}^{J/\psi}}{N_{J/\psi} + \rho_{0,0}^{J/\psi}}, \\ \lambda_{\phi'}^{J/\psi} &= \frac{2\Re(\rho_{1,-1}^{J/\psi})}{N_{J/\psi} + \rho_{0,0}^{J/\psi}}, \\ \lambda_{\theta' \phi'}^{J/\psi} &= \frac{\sqrt{2}(\Re(\rho_{1,0}^{J/\psi}) - \Re(\rho_{-1,0}^{J/\psi}))}{N_{J/\psi} + \rho_{0,0}^{J/\psi}}, \\ \lambda_{\theta' \phi'}^{\perp J/\psi} &= -\frac{2\Im(\rho_{1,-1}^{J/\psi})}{N_{J/\psi} + \rho_{0,0}^{J/\psi}}, \\ \lambda_{\theta' \phi'}^{\perp J/\psi} &= -\frac{\sqrt{2}(\Im(\rho_{1,0}^{J/\psi}) + \Im(\rho_{-1,0}^{J/\psi}))}{N_{J/\psi} + \rho_{0,0}^{J/\psi}}, \end{aligned} \quad (16)$$

the expressions in Eq.(13) are recovered.

In the second scenario, \vec{s}_2^z is chosen as the same as \vec{s}_1^z . The spin eigenstate $|1, s_z\rangle$ with respect to \vec{s}_2^z for the J/ψ is no longer its helicity state like in the first scenario.

¹ Note, we use general vector current amplitudes for the J/ψ decays into a muon pair.

² Note, it is just the case of the J/ψ feed-down from the χ_{cJ} decay.

With a direct calculation following Eq.(12), we obtain

$$\begin{aligned}
\lambda_{\theta'}^{\chi_{c1}} &= \frac{-N_{\chi_{c1}} + 3\rho_{0,0}^{\chi_{c1}}}{3N_{\chi_{c1}} - \rho_{0,0}^{\chi_{c1}}}, \\
\lambda_{\phi'}^{\chi_{c1}} &= -\frac{2\Re\rho_{1,-1}^{\chi_{c1}}}{3N_{\chi_{c1}} - \rho_{0,0}^{\chi_{c1}}}, \\
\lambda_{\theta'\phi'}^{\chi_{c1}} &= -\frac{\sqrt{2}(\Re\rho_{1,0}^{\chi_{c1}} - \Re\rho_{-1,0}^{\chi_{c1}})}{3N_{\chi_{c1}} - \rho_{0,0}^{\chi_{c1}}}, \\
\lambda_{\phi'}^{\perp\chi_{c1}} &= \frac{2\Im\rho_{1,-1}^{\chi_{c1}}}{3N_{\chi_{c1}} - \rho_{0,0}^{\chi_{c1}}}, \\
\lambda_{\theta'\phi'}^{\perp\chi_{c1}} &= \frac{\sqrt{2}(\Im\rho_{1,0}^{\chi_{c1}} + \Im\rho_{-1,0}^{\chi_{c1}})}{3N_{\chi_{c1}} - \rho_{0,0}^{\chi_{c1}}}, \\
\lambda_{\theta'}^{\chi_{c2}} &= \frac{6N_{\chi_{c2}} - 9(\rho_{1,1}^{\chi_{c2}} + \rho_{-1,-1}^{\chi_{c2}}) - 12\rho_{0,0}^{\chi_{c2}}}{6N_{\chi_{c2}} + 3(\rho_{1,1}^{\chi_{c2}} + \rho_{-1,-1}^{\chi_{c2}}) + 4\rho_{0,0}^{\chi_{c2}}}, \\
\lambda_{\phi'}^{\chi_{c2}} &= \frac{2\sqrt{6}(\Re\rho_{2,0}^{\chi_{c2}} + \Re\rho_{-2,0}^{\chi_{c2}}) + 6\Re\rho_{1,-1}^{\chi_{c2}}}{6N_{\chi_{c2}} + 3(\rho_{1,1}^{\chi_{c2}} + \rho_{-1,-1}^{\chi_{c2}}) + 4\rho_{0,0}^{\chi_{c2}}}, \\
\lambda_{\theta'\phi'}^{\chi_{c2}} &= \frac{6(\Re\rho_{2,1}^{\chi_{c2}} - \Re\rho_{-2,-1}^{\chi_{c2}}) + \sqrt{6}(\Re\rho_{1,0}^{\chi_{c2}} - \Re\rho_{-1,0}^{\chi_{c2}})}{6N_{\chi_{c2}} + 3(\rho_{1,1}^{\chi_{c2}} + \rho_{-1,-1}^{\chi_{c2}}) + 4\rho_{0,0}^{\chi_{c2}}}, \\
\lambda_{\phi'}^{\perp\chi_{c2}} &= \frac{2\sqrt{6}(\Im\rho_{0,2}^{\chi_{c2}} - \Im\rho_{0,-2}^{\chi_{c2}}) - 6\Im\rho_{1,-1}^{\chi_{c2}}}{6N_{\chi_{c2}} + 3(\rho_{1,1}^{\chi_{c2}} + \rho_{-1,-1}^{\chi_{c2}}) + 4\rho_{0,0}^{\chi_{c2}}}, \\
\lambda_{\theta'\phi'}^{\perp\chi_{c2}} &= \frac{6(\Im\rho_{1,2}^{\chi_{c2}} + \Im\rho_{-1,-2}^{\chi_{c2}}) + \sqrt{6}(\Im\rho_{0,1}^{\chi_{c2}} + \Im\rho_{0,-1}^{\chi_{c2}})}{6N_{\chi_{c2}} + 3(\rho_{1,1}^{\chi_{c2}} + \rho_{-1,-1}^{\chi_{c2}}) + 4\rho_{0,0}^{\chi_{c2}}}.
\end{aligned} \tag{17}$$

One can also derive them by combining

$$\begin{aligned}
\rho_{s_z, s'_z}^{\chi_{cJ} \rightarrow J/\psi \gamma} &\propto \sum_{l_z = \pm 1, 0} \sum_{J_z, J'_z} \langle 1, l_z; 1, s_z | J, J_z \rangle \\
&\langle J, J'_z | 1, l_z; 1, s'_z \rangle \rho_{J_z, J'_z}^{\chi_{cJ}} \text{Br}(\chi_{cJ} \rightarrow J/\psi \gamma), \tag{18}
\end{aligned}$$

and Eq.(16). The expressions in the scenario are also exactly the same as those in Ref.[24]. It is interesting to see that these observables are mildly corrected by the additional M2 and E3 transitions.

Similarly, one is able to use the same procedure to derive the formulas for other scenarios.

VI. DETERMINATION OF $\rho_{J_z, J'_z}(|J_z - J'_z| > 2)$ FOR χ_{c2} WITH REWEIGHTING METHOD

From Eqs.(11,13,17), we find that the SDMEs $\rho_{J_z, J'_z}(|J_z - J'_z| > 2)$ of χ_{c2} cannot be measured from these angular distributions. The fact that the coefficients of these SDMEs are suppressed by v^2 or $(m_{\chi_{c2}} - m_{J/\psi})$ makes the measurement of these polarization observables difficult. In this section, we propose a reweighting method to measure these SDMEs.

From Eq.(9), one can see that this fact is the origin for the cancelation of the transverse J/ψ and the longitudinal J/ψ from the χ_{c2} decay. If the probabilities of

the transverse and the longitudinal parts are made different by reweighting, we will have opportunity to split $\rho_{J_z, J'_z}(|J_z - J'_z| > 2)$ without any suppressions. The only tradeoff is that one should also measure the polar angle θ' of the μ^+ from the J/ψ subsequent decay³. As is well known, the polar angular distribution of the μ^+ from the transverse polarized J/ψ decay is $\frac{(1+\cos^2\theta')}{2}$, while that from the longitudinal one is $(1 - \cos^2\theta')$. Therefore, after integrating over solid angles of the μ^+ , the weights for the transverse and longitudinal J/ψ are equal, i.e. $D_{J_z, J'_z} = \sum_{\lambda_{J/\psi}=\pm, 0, \lambda_\gamma=\pm} \mathcal{M}_{J_z, \lambda_{J/\psi}, \lambda_\gamma} \mathcal{M}_{J'_z, \lambda_{J/\psi}, \lambda_\gamma}^*$, and it then results in the cancelation of those two parts in $\rho_{J_z, J'_z}(|J_z - J'_z| > 2)$ of χ_{c2} . In order to avoid these cancelations, a direct way is to measure the θ' of the μ^+ and then assign every reconstructed μ^+ event from $\chi_{c2} \rightarrow J/\psi \gamma \rightarrow \mu^+ \mu^- \gamma$ an extra weight $w(\cos^2\theta')$. For example, if one chooses $w(\cos^2\theta') \propto \cos^2\theta'$, because of

$$\begin{aligned}
&\int d\cos\theta' (1 - \cos^2\theta') w(\cos^2\theta') \\
&: \int d\cos\theta' \frac{(1 + \cos^2\theta')}{2} w(\cos^2\theta') = 1 : 2,
\end{aligned}$$

the decay SDMEs become

$$\begin{aligned}
D_{J_z, J'_z} &= 2 \sum_{\lambda_{J/\psi}=\pm, \lambda_\gamma=\pm} \mathcal{M}_{J_z, \lambda_{J/\psi}, \lambda_\gamma} \mathcal{M}_{J'_z, \lambda_{J/\psi}, \lambda_\gamma}^* \\
&+ \sum_{\lambda_\gamma=\pm} \mathcal{M}_{J_z, 0, \lambda_\gamma} \mathcal{M}_{J'_z, 0, \lambda_\gamma}^*, \tag{19}
\end{aligned}$$

and the cancelations do not occur. Without losing generalization, we assume that

$$\begin{aligned}
&\int d\cos\theta' (1 - \cos^2\theta') w(\cos^2\theta') \\
&: \int d\cos\theta' \frac{(1 + \cos^2\theta')}{2} w(\cos^2\theta') = r_L : r_T,
\end{aligned}$$

and

$$\begin{aligned}
D_{J_z, J'_z} &= r_T \sum_{\lambda_{J/\psi}=\pm, \lambda_\gamma=\pm} \mathcal{M}_{J_z, \lambda_{J/\psi}, \lambda_\gamma} \mathcal{M}_{J'_z, \lambda_{J/\psi}, \lambda_\gamma}^* \\
&+ r_L \sum_{\lambda_\gamma=\pm} \mathcal{M}_{J_z, 0, \lambda_\gamma} \mathcal{M}_{J'_z, 0, \lambda_\gamma}^*. \tag{20}
\end{aligned}$$

Hence, the angular distribution of J/ψ from the χ_{c2} de-

³ Note that we are permitted to assume the z axis is in the flight direction of J/ψ in the rest frame of χ_{c2} .

cay is

$$\begin{aligned}
\tilde{W}^{\chi_{c2} \rightarrow J/\psi \gamma}(\theta, \phi) \propto & 1 + \lambda_\theta \cos^2 \theta + \lambda_{2\theta} \cos^4 \theta \\
& + \lambda_\phi \sin^2 \theta \cos 2\phi + \lambda_\phi^\perp \sin^2 \theta \sin 2\phi \\
& + \lambda_{\theta\phi} \sin 2\theta \cos \phi + \lambda_{\theta\phi}^\perp \sin 2\theta \sin \phi \\
& + \lambda_{2\phi} \sin^4 \theta \cos 2\phi + \lambda_{2\phi}^\perp \sin^4 \theta \sin 2\phi \\
& + \lambda_{2\theta\phi} \sin 2\theta \sin^2 \theta \cos \phi \\
& + \lambda_{2\theta\phi}^\perp \sin 2\theta \sin^2 \theta \sin \phi \\
& + \lambda_{3\theta\phi} \sin 2\theta \sin^2 \theta \cos 3\phi \\
& + \lambda_{3\theta\phi}^\perp \sin 2\theta \sin^2 \theta \sin 3\phi \\
& + \lambda_{4\phi} \sin^4 \theta \cos 4\phi \\
& + \lambda_{4\phi}^\perp \sin^4 \theta \sin 4\phi.
\end{aligned} \tag{21}$$

The explicit expressions for the coefficients are

$$\begin{aligned}
N_{\chi_{c2}} &= \rho_{2,2} + \rho_{1,1} + \rho_{0,0} + \rho_{-1,-1} + \rho_{-2,-2}, \\
R &= 3(r_T + r_L)N_{\chi_{c2}} + 3r_T(\rho_{1,1} + \rho_{-1,-1}) + (7r_T - 3r_L)\rho_{0,0}, \\
\lambda_\theta &= \frac{6r_T N_{\chi_{c2}} - 9r_L(\rho_{1,1} + \rho_{-1,-1}) - 6(5r_T - 3r_L)\rho_{0,0}}{R}, \\
\lambda_{2\theta} &= (r_T - r_L) \frac{3N_{\chi_{c2}} - 15(\rho_{1,1} + \rho_{-1,-1}) + 15\rho_{0,0}}{R},
\end{aligned}$$

$$\begin{aligned}
\lambda_\phi &= \left[2\sqrt{6}(4r_T - 3r_L)(\Re\rho_{2,0} + \Re\rho_{-2,0}) \right. \\
&\quad \left. - 6(2r_T - 3r_L)\Re\rho_{1,-1} \right] / R, \\
\lambda_\phi^\perp &= - \left[2\sqrt{6}(4r_T - 3r_L)(\Im\rho_{2,0} - \Im\rho_{-2,0}) \right. \\
&\quad \left. - 6(2r_T - 3r_L)\Im\rho_{1,-1} \right] / R, \\
\lambda_{\theta\phi} &= \left[6(2r_T - r_L)(\Re\rho_{2,1} - \Re\rho_{-2,-1}) \right. \\
&\quad \left. - \sqrt{6}(2r_T - 3r_L)(\Re\rho_{1,0} - \Re\rho_{-1,0}) \right] / R, \\
\lambda_{\theta\phi}^\perp &= - \left[6(2r_T - r_L)(\Im\rho_{2,1} + \Im\rho_{-2,-1}) \right. \\
&\quad \left. - \sqrt{6}(2r_T - 3r_L)(\Im\rho_{1,0} + \Im\rho_{-1,0}) \right] / R, \\
\lambda_{2\phi} &= (r_T - r_L) \frac{24\Re\rho_{1,-1} - 6\sqrt{6}(\Re\rho_{2,0} + \Re\rho_{-2,0})}{R}, \\
\lambda_{2\phi}^\perp &= -(r_T - r_L) \frac{24\Im\rho_{1,-1} - 6\sqrt{6}(\Im\rho_{2,0} - \Im\rho_{-2,0})}{R}, \\
\lambda_{2\theta\phi} &= 6(r_T - r_L) \left[-(\Re\rho_{2,1} - \Re\rho_{-2,-1}) \right. \\
&\quad \left. + \sqrt{6}(\Re\rho_{1,0} - \Re\rho_{-1,0}) \right] / R, \\
\lambda_{2\theta\phi}^\perp &= 6(r_T - r_L) \left[(\Im\rho_{2,1} + \Im\rho_{-2,-1}) \right. \\
&\quad \left. - \sqrt{6}(\Im\rho_{1,0} + \Im\rho_{-1,0}) \right] / R, \\
\lambda_{3\theta\phi} &= 6(r_T - r_L) \frac{\Re\rho_{2,-1} - \Re\rho_{-2,1}}{R}, \\
\lambda_{3\theta\phi}^\perp &= -6(r_T - r_L) \frac{\Im\rho_{2,-1} + \Im\rho_{-2,1}}{R}, \\
\lambda_{4\phi} &= (r_T - r_L) \frac{6\Re\rho_{2,-2}}{R}, \\
\lambda_{4\phi}^\perp &= -(r_T - r_L) \frac{6\Im\rho_{2,-2}}{R}.
\end{aligned} \tag{22}$$

From the above equations, we find that one can measure $\lambda_{3\theta\phi}$, $\lambda_{3\theta\phi}^\perp$, $\lambda_{4\phi}$, $\lambda_{4\phi}^\perp$ to determine the values of $\rho_{J_z, J_z'} (|J_z -$

$J_z'| > 2)$ if $r_T \neq r_L$. It is also interesting to note that using the re-weighting method, we are not only able to extract $\rho_{J_z, J_z'} (|J_z - J_z'| > 2)$, but also have the chance to determine all of the SDMEs, which is not met in Eq.(11). For the measurement of the muon angular distribution from the χ_{c2} decay, the similar weight $w(\cos^2 \theta)$ can be assigned to every event in the rest frame of the χ_{c2} . Combining the measurements with different weights, one may also have opportunity to extract all of the production SDMEs of χ_{c2} in the investigation of the production mechanism. At the end of this section, we want to point out that the reweighting method is also useful in the extraction of the coefficients in Eq.(21) on the experimental side when one does an 1-dimensional bin fitting rather than the 2-dimensional bin fitting. A weight $w(\cos^2 \theta)$ (e.g. $w(\cos^2 \theta) = \cos^2 \theta$) can be applied to separate λ_ϕ , $\lambda_{2\phi}$ and $\lambda_{\theta\phi}$, $\lambda_{2\theta\phi}$.

VII. ROTATION INVARIANT RELATIONS FOR ARBITRARY SPIN-INTEGGER PARTICLES

The partonic Drell-Yan process in perturbative QCD obeys the well-know Lam-Tung identity[30], which states that the coefficients λ_θ and λ_ϕ of the lepton angular distribution from the Drell-Yan process satisfy $\lambda_\theta + 4\lambda_\phi = 1$. Its theoretical relevance is that the relation remains unchanged up to $\mathcal{O}(\alpha_s^2)$ corrections[31] and receives relatively small corrections even by resummation[32]. The distinctive feature of the identity is also independent of the chosen orientation of the spin axis. Later it was pointed out that the rotation invariance of Lam-Tung relation is a general consequence of the rotational covariance of $J = 1$ angular momentum eigenstates by the authors of [33]. They presented an expression formally analogous to the Lam-Tung identity for a $J = 1$ boson decays into a fermion pair with the only assumption that the spin-quantization axis \vec{s} should be set in the production plane, i.e. $F_1 = \frac{1+\lambda_\theta+2\lambda_\phi}{3+\lambda_\theta}$. The new observable F_1 is rotation invariant in the production plane. The condition that the spin-quantization axis is in the production plane is indeed fulfilled in HX, the Collins-Soper frame, the Gottfried-Jackson frame and the target frame. From Ref.[33], we know that the rotation-invariant property of F_1 is guaranteed from a relation of the Wigner functions $d_{1,M}^1(\theta) + d_{-1,M}^1(\theta) = \delta_{|M|,1}$. In the section, we want to generalize the relation to the arbitrary spin-n (n is an integer) particles. We straightforwardly write down the

linear identities for the Wigner functions:

$$\begin{aligned}
& \sum_{m=-k}^k \langle k, m; k, m | 2k, 2m \rangle d_{2m, M}^{2k}(\theta) \\
&= \langle k, \frac{M}{2}; k, \frac{M}{2} | 2k, M \rangle \delta_{\text{mod}(M, 2), 0}, \quad n = 2k, \\
& \sum_{m=0}^k \langle 2k+1-m, 0; m, 0 | 2k+1, 0 \rangle \\
& (d_{2k+1-m, M}^{2k+1}(\theta) + d_{m-2k-1, M}^{2k+1}(\theta)) \\
&= \langle \frac{|M|+1}{2} + k, 0; \frac{1-|M|}{2} + k, 0 | 2k+1, 0 \rangle \\
& \delta_{\text{mod}(M, 2), 1}, \quad n = 2k+1, \quad (23)
\end{aligned}$$

where k is a non-negative integer. The amplitudes with respect to a chosen polarization axis can be symbolically denoted as $|n\rangle = \sum_{m=-n}^n a_m |n, m\rangle$, where $|n, m\rangle$ is an J_z eigenstates with the eigenvalues $m = -n, -n+1, \dots, n$, and a_m is the production amplitude, i.e. $\rho_{J_z, J'_z} \equiv a_{J_z} a_{J'_z}^*$. From Eq.(23), we can immediately draw a conclusion that the linear combinations of amplitudes

$$b_{2k} \equiv \sum_{m=-k}^k \langle k, m; k, m | 2k, 2m \rangle a_{2m}, \text{ when } n = 2k,$$

and

$$\begin{aligned}
b_{2k+1} &\equiv \sum_{m=0}^k \langle 2k+1-m, 0; m, 0 | 2k+1, 0 \rangle \\
& (a_{2k+1-m} + a_{m-1-2k}), \text{ when } n = 2k+1,
\end{aligned}$$

are invariant under the rotation in the production plane. Therefore, the observables like F_n defined as

$$\begin{aligned}
F_n &\equiv \frac{1}{B_n} \frac{|b_n|^2}{N_n}, \\
N_n &\equiv \sum_{m=-n}^n |a_m|^2 \equiv \sum_{m=-n}^n \rho_{m, m}, \quad (24)
\end{aligned}$$

are rotation-invariant, where B_n is a normalization factor to ensure $0 \leq F_n \leq 1$. Or in a more extended sense, the functions of F_n are rotation-invariant. The F_n can be expressed into the rational functions of the coefficients in the particles' decay products' angular distributions (e.g., $\lambda_\theta, \lambda_\phi$, etc). Specifically, for the spin-1 particles, the observable is

$$F_1 \equiv \frac{1}{2} \frac{|a_1 + a_{-1}|^2}{|a_1|^2 + |a_0|^2 + |a_{-1}|^2}, \quad (25)$$

while for the spin-2 particles, its expression is

$$F_2 \equiv \frac{1}{3} \frac{|a_2 + \sqrt{\frac{2}{3}} a_0 + a_{-2}|^2}{|a_2|^2 + |a_1|^2 + |a_0|^2 + |a_{-1}|^2 + |a_{-2}|^2}. \quad (26)$$

Two concise examples of F_1 are the J/ψ decays into two muons and the χ_{c1} decays into a J/ψ and a photon. For the J/ψ ,

$$F_1^{J/\psi \rightarrow \mu^+ \mu^-} = \frac{1 + \lambda_{\theta'} + 2\lambda_{\phi'}}{3 + \lambda_{\theta'}}, \quad (27)$$

which has been presented in Ref.[33], while for the χ_{c1} , one can derive

$$F_1^{\chi_{c1} \rightarrow J/\psi \gamma} = \frac{1 - \lambda_\theta - 4\lambda_\phi}{3 + \lambda_\theta} \quad (28)$$

from Eqs.(7,25). The χ_{c2} provides an example of the spin-2 particles. In fact, the complete angular distribution of the χ_{c2} 's decay product J/ψ is Eq.(21) instead of Eq.(10). However, the terms absent in Eq.(10) are suppressed as mentioned above. Hence, the spin information in Eq.(11) is not sufficient. We have proposed a method to extract the full spin information of the χ_{c2} in the last section. With Eq.(22) and Eq.(26), one obtains

$$\begin{aligned}
F_2^{\chi_{c2} \rightarrow J/\psi \gamma} &= \frac{n_1 + n_2 \lambda_\theta + n_3 \lambda_{2\theta} + n_4 \lambda_\phi + n_5 \lambda_{2\phi} + n_6 \lambda_{4\phi}}{d_1 + d_2 \lambda_\theta + d_3 \lambda_{2\theta}}, \\
n_1 &= \frac{2}{3}, \\
n_2 &= \frac{2(8r_T + r_L)}{3(10r_T - 3r_L)}, \\
n_3 &= \frac{6r_T^2 - 3r_T r_L - r_L^2}{(10r_T - 3r_L)(r_T - r_L)}, \\
n_4 &= \frac{4(7r_T + 3r_L)}{3(10r_T - 3r_L)}, \\
n_5 &= \frac{(2r_T - 3r_L)(7r_T + 3r_L)}{3(10r_T - 3r_L)(r_T - r_L)}, \\
n_6 &= \frac{7r_T + 3r_L}{3(r_T - r_L)}, \\
d_1 &= \frac{15}{4}, d_2 = \frac{5}{4}, d_3 = \frac{3}{4}. \quad (29)
\end{aligned}$$

In particular, if the weight $w(x) = x$, then $r_T = 2, r_L = 1$ and

$$F_2^{\chi_{c2} \rightarrow J/\psi \gamma} = \frac{4}{3} \frac{2 + 2\lambda_\theta + 3\lambda_{2\theta} + 4\lambda_\phi + \lambda_{2\phi} + 17\lambda_{4\phi}}{15 + 5\lambda_\theta + 3\lambda_{2\theta}}. \quad (30)$$

These frame-invariant relations can be extended to the study of other bosons or mesons. We also suggest the experimentalists to measure these observables to make a cross-check of their extractions of the angular distribution coefficients in different frames.

VIII. UNCERTAINTY OF J/ψ POLARIZATION FROM FEED-DOWN

The CDF data for the J/ψ prompt production include not only direct J/ψ production but also the feed-down

contributions from χ_{cJ} and ψ' . However, the recent NLO calculations of J/ψ polarization both in Ref.[19] and Ref.[18] are devoid of the feed-down contributions. Though the LO NRQCD prediction of the feed-down to the J/ψ polarization in [34] was found to have a minor impact on the final LO result, one may still doubt whether the NLO feed-down effect on $\lambda_{\theta'}^4$ of the J/ψ can be neglected since the NLO correction to the P-wave is large[8]. In this section, we will estimate the possible uncertainty of the J/ψ polarization $\lambda_{\theta'}$ arising from the feed-down of the χ_c and ψ' decays.

The calculation of the prompt J/ψ is a little complicated. In general, prompt data are composed of four parts, i.e. the direct production of the J/ψ , the single-cascade decay of the χ_c and the ψ' and the double cascade decay of $\psi' \rightarrow \chi_c \gamma \rightarrow J/\psi \gamma \gamma$. The direct production of the J/ψ is straightforward as has been done e.g. in Refs.[18, 19]. Relation between the production SDMEs of the χ_c and the production SDMEs of the J/ψ from the χ_c decay has been given in Eq.(18), while the relation between the production SDMEs of the ψ' and those of the χ_c from the ψ' decay is

$$\rho_{J_z, J_z'}^{\psi' \rightarrow \chi_{cJ}} \propto \sum_{l_z, s_z, s_z' = \pm 1, 0} \langle 1, l_z; 1, s_z | J, J_z \rangle \langle 1, l_z; 1, s_z' | J, J_z' \rangle \rho_{s_z, s_z'}^{\psi'} \quad (31)$$

Combine Eq.(31) and Eq.(18), the double-cascade decay component can also be calculated. At last, the single-cascade decay of the ψ' contribution to the J/ψ can be treated the same as the $S_1^{[8]}$ to the J/ψ , because of the same selection rule in the electromagnetic dipole transition and the chromomagnetic dipole transition. One can easily verify it that the above procedure gives the same formula as in Ref.[34].

Next, we just divide the contribution of the prompt J/ψ as the direct part ρ^d , which we already know at the NLO level and the unknown feed-down part ρ^f . We assume the polarization observables as $\lambda_{\theta'}^d$ and $\lambda_{\theta'}^f$ respectively. Moreover, the fraction of the J/ψ cross section from the feed-down respect to the prompt cross section is denoted as r , i.e. $r \equiv \frac{2\rho_{1,1}^f + \rho_{0,0}^f}{2\rho_{1,1}^d + \rho_{0,0}^d}$ with $\rho_{s_z, s_z'} \equiv \rho_{s_z, s_z'}^f + \rho_{s_z, s_z'}^d$ and $\rho \equiv 2\rho_{1,1} + \rho_{0,0}$. Hence,

$$\begin{aligned} \rho_{0,0}^f &= r \frac{1 - \lambda_{\theta'}^f}{3 + \lambda_{\theta'}^f} \rho, \quad \rho_{1,1}^f = r \frac{1 + \lambda_{\theta'}^f}{3 + \lambda_{\theta'}^f} \rho, \\ \rho_{0,0}^d &= (1-r) \frac{1 - \lambda_{\theta'}^d}{3 + \lambda_{\theta'}^d} \rho, \quad \rho_{1,1}^d = (1-r) \frac{1 + \lambda_{\theta'}^d}{3 + \lambda_{\theta'}^d} \rho \end{aligned} \quad (32)$$

⁴ Note, to be consistent throughout the context, the polarization observables of the J/ψ or the angular distributions of the muon are all denoted by an extra prime.

⁵ Note that we use the symmetry property $\rho_{-\lambda, -\lambda'}^H = (-)^{\lambda - \lambda'} \rho_{\lambda, \lambda'}^H$ in hadroproduction which is guaranteed by parity invariance[35].

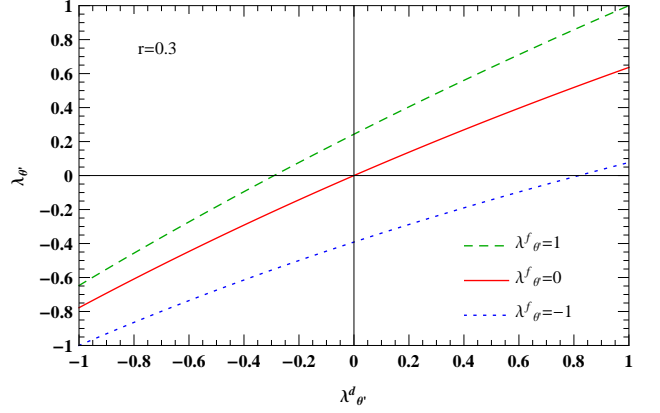


FIG. 1: Possible impact of the feed-down on the prompt J/ψ polar asymmetry polarization $\lambda_{\theta'}$ with respect to various direct J/ψ polarization $\lambda_{\theta'}^d$. Here $r = 0.3$ is assumed, and the curves correspond to J/ψ polarizations from the feed-down $\lambda_{\theta'}^f = \pm 1, 0$.

and

$$\lambda_{\theta'} = \frac{r \lambda_{\theta'}^f}{3 + \lambda_{\theta'}^f} + \frac{(1-r) \lambda_{\theta'}^d}{3 + \lambda_{\theta'}^d} \quad (33)$$

Two specific cases are analyzed firstly, i.e. $\lambda_{\theta'}^d = 0$ and $\lambda_{\theta'}^d = 1$, which are the approximated values of the J/ψ polarization at the Tevatron in HX in Ref.[8] and Ref.[18] in $p_T > 10\text{GeV}$ regime respectively. We obtained the polarization of the prompt J/ψ as $-\frac{3r}{2+r} \leq \lambda_{\theta'} \leq \frac{3r}{4-r}$ and $\frac{2-6r}{2+2r} \leq \lambda_{\theta'} \leq 1$ when varying $\lambda_{\theta'}^f$ from -1 to 1 . If we just take $r = 0.3$, which is the usually used value by people, the feed-down contribution may change $\lambda_{\theta'}$ from 0.24 to -0.39 when $\lambda_{\theta'}^d = 0$ and from 1 to 0.08 when the polarization of the direct J/ψ is fully transverse. Hence, it seems the impact of the feed-down is more significant in polarization prediction in Ref.[18] than in Ref.[19] especially when $\lambda_{\theta'} = -1$. Thus far, the main conclusion in Ref.[19] is expected to be not changed too much even after including the feed-down contributions as long as we use the same LDMEs. In Fig.(1), we establish the curves of $\lambda_{\theta'}$ with respect to $\lambda_{\theta'}^d$ with $\lambda_{\theta'}^f = \pm 1, 0$ with $r = 0.3$. The prompt J/ψ polarization $\lambda_{\theta'}$ can only be within the upper and lower curves. Fig.2 shows the impact of the feed-down from the χ_c and the ψ' decay into the prompt J/ψ polarization $\lambda_{\theta'}$ in HX at the Tevatron with $\sqrt{S} = 1.96\text{TeV}$ and $|y_{J/\psi}| < 0.6$. The values of LDMEs are demonstrated in Tab.I, which is obtained by fitting the NLO result with the Tevatron data in Ref.[19]. Only central value of the direct J/ψ polarization is plotted. From this figure, we see the feed-down of χ_c and ψ' do not change our result much and our conclusion in Ref.[19] is still valid.

$\langle \mathcal{O}^{J/\psi}(S_1^{[1]}) \rangle$ GeV ³	$\langle \mathcal{O}^{J/\psi}(S_0^{[8]}) \rangle$ 10 ⁻² GeV ³	$\langle \mathcal{O}^{J/\psi}(S_1^{[8]}) \rangle$ 10 ⁻² GeV ³	$\langle \mathcal{O}^{J/\psi}(P_0^{[8]}) \rangle/m_c^2$ 10 ⁻² GeV ³
1.16	8.9	0.30	0.56

TABLE I: CO LDMEs for J/ψ from Ref.[19], which is obtained by fitting the differential cross section and polarization of prompt J/ψ simultaneously at the Tevatron [5]. The CS LDME is calculated by the B-T potential model in Ref.[36].

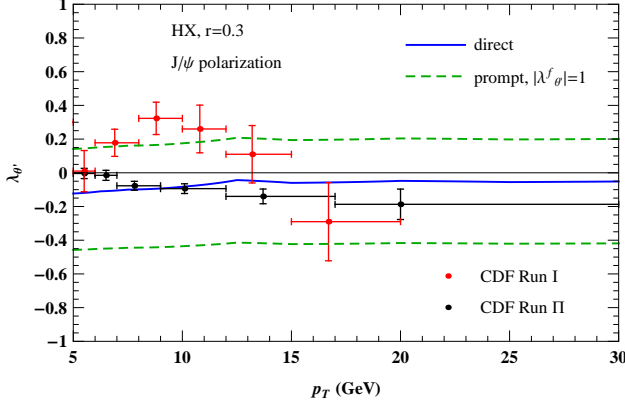


FIG. 2: The J/ψ polar asymmetry polarization $\lambda_{\theta'}$ in HX at the Tevatron with the LDMEs in Tab.I. The dashed lines represent the upper and lower limits of the possible feed-down contribution to $\lambda_{\theta'}$ with $r = 0.3$. CDF data are taken from Refs.[4, 5].

IX. PHENOMENOLOGY

In this section, we are now in a position to present our results for the inclusive χ_{c1} and χ_{c2} production at the LHC with $\sqrt{S} = 8\text{TeV}$. We also present individual Fock states' contributions to SDMEs for the convenience to the readers who want to use different LDMEs by using our results with simple re-scaling.

We use our automatic matrix element generator of the heavy quarkonium amplitudes to calculate all of the SDMEs under various conditions. The generator is built up after we rewrote the core codes of the published HELAC[37, 38], PHEGAS[39, 40], RAMBO[41] and VEGAS[42]. The program has been tested by a number of benchmark processes and has been used in the calculation of J/ψ polarization successfully[19].

The input parameters in our calculations are:

- 1) $m_c = 1.5\text{GeV}, m_{\chi_c} = 2m_c = 3\text{GeV}$.
- 2) $\sqrt{S} = 8\text{TeV}, |y_{\chi_c}| < 2.4$.
- 3) PDF set is CTEQ6L1[43].
- 4) $\mu_r = \mu_f = \sqrt{(2m_c)^2 + p_T^2}$.
- 5) $\langle \mathcal{O}^{\chi_{cJ}}(P_J^{[1]}) \rangle = \frac{3(2J+1)2N_c}{4\pi} |R'_P(0)|^2$, with $|R'_P(0)|^2 = 0.075\text{GeV}^5[36]$, $\frac{\langle \mathcal{O}^{\chi_{cJ}}(S_1^{[8]}) \rangle}{2J+1} = 2.2 \times 10^{-3}\text{GeV}^3[8]$.

The relations between SDMEs of $S_1^{[8]}$ and those of $P_J^{[1]}$ are similar as in Eq.(31) and are specifically

$$\rho_{J_z, J'_z}^{S_1^{[8]} \rightarrow \chi_{cJ}} \propto \sum_{l_z, s_z, s'_z = \pm 1, 0} \langle 1, l_z; 1, s_z | J, J_z \rangle \langle 1, l_z; 1, s'_z | J, J'_z \rangle \rho_{s_z, s'_z}^{S_1^{[8]}} \quad (34)$$

Fig.(3), Fig.(4) and Fig.(5) present the transverse momentum distributions of $\frac{d\sigma_{00}}{dp_T}$ and $\frac{d\sigma_{11}}{dp_T}$ for $P_1^{[1]}$, $P_2^{[1]}$ and $S_1^{[8]}$ respectively in HX, the Collins-Soper, the Gottfried-Jackson and the target frames. For $P_2^{[1]}$, there is $\frac{d\sigma_{22}}{dp_T}$ contribution too. The cross section in each channel ($\frac{d\sigma_{\text{tot}}}{dp_T} = 2\frac{d\sigma_{11}}{dp_T} + \frac{d\sigma_{00}}{dp_T}$ for $P_1^{[1]}$ and $S_1^{[8]}$, $\frac{d\sigma_{\text{tot}}}{dp_T} = 2\frac{d\sigma_{22}}{dp_T} + 2\frac{d\sigma_{11}}{dp_T} + \frac{d\sigma_{00}}{dp_T}$ for $P_2^{[1]}$) is also presented, which will be used in the normalization of the non-diagonal SDMEs in Figs.(6,7,8). We should stress one point that in Fig.(5) only $\langle \mathcal{O}^{\chi_{c0}}(S_1^{[8]}) \rangle = 2.2 \times 10^{-3}\text{GeV}^3$ are used. In the rest of the figures, we demonstrate the angular distribution observables derived in Eqs.(7,11,13), where besides NRQCD predictions, the CS components are also demonstrated. The results show that CO makes a significant change compared to the result with CS only.

Some features should be emphasized:

1) From the curves of the total cross sections in Figs.(3,4,5), we may conclude that the CS dominates in the low transverse momentum region, while the CO may dominate when p_T increases because gluon fragmentation processes[44] become important. The CS p_T distribution may receive significant contributions from the higher order radiative corrections[8]. The full NLO predictions for χ_{cJ} polarizations will be presented later.

2) From Figs.(3,4,5,6,7,8), we observe that the results of $\rho_{i,j}$ in the Gottfried-Jackson frame and the target frame coincide within error bars, aside from a factor $(-1)^{i-j}$, which is also pointed out in Ref.[23]. For diagonal elements, i.e. $\rho_{i,i}$, the curves in the Gottfried-Jackson and the target frames are similar to those in the helicity frame, while many distinctions are found in the Collins-Soper frame. Hence for the polarization observable λ_θ , the helicity and the Collins-Soper frames are enough. Moreover, from Fig.(5), we see that the longitudinal cross section of the $S_1^{[8]}$ channel is the largest in the Collins-Soper frame when $p_T \gg 2m_c$, which is consistent with the statement in Ref.[45].

3) In the helicity and the Collins-Soper frames, the SDMEs $\rho_{i,j}$ with $|i-j|$ odd are almost zero. Therefore, they should be measured in the Gottfried-Jackson and the target frames as well as $\lambda_{\theta\phi}$ and $\lambda_{\theta'\phi'}$ shown in Figs.(11,14,15,17). For $\rho_{i,j}$ with $|i-j|$ even, the measurements in the helicity and the Collins-Soper frames are much better than in the Gottfried-Jackson and the target frames.

4) In Figs.(15,16,17), we only consider the first scenario

in the previous section, i.e. Eq.(13)⁶. In this scenario, the E1 transition just predicts fixed values of $\lambda_{\theta'}^{\chi_{c1}}$, $\lambda_{\phi'}^{\chi_{c1}}$ and $\lambda_{\theta'}^{\chi_{c2}}$. On the experimental sides, one can measure these observables to see the contributions of suppressed transitions like the M2 and E3 parts. These precision measurements will improve the test of the validation of NRQCD factorization.

5) The observables defined in Eqs.(25,26) for the χ_{c1} and the χ_{c2} are shown in Fig.(18). The figures show that these observables are indeed frame-independent. Hence, it would be interesting to measure these observables at the LHC.

X. SUMMARY

Finally, we draw our conclusion. The upgrade of the integrated luminosity at the LHC will not only allow us to measure the polarizations of S -wave quarkonium states like J/ψ and ψ' , but also the angular distributions of decay products from the P -wave states χ_{cJ} . This has opened up new opportunities to further test NRQCD factorization and quarkonium production mechanisms in general. In this paper, we present a general framework to investigate the polarizations of χ_{cJ} and to study the impact of these P -wave states to the polarization of J/ψ by considering the decay vertex functions. Specifically, we derive the polar and azimuthal angle distributions of the J/ψ produced from the χ_{c1} and χ_{c2} decays and the muon produced from the cascade decay $\chi_{cJ} \rightarrow J/\psi \gamma \rightarrow \mu^+ \mu^- \gamma$. The coefficients of angular distributions, which preserve the spin information of the χ_{cJ} , are expressed in terms of rational functions of the χ_{cJ} production SDMEs in Eqs.(7,11,13,17,22). We also derive the rotation-invariant relations Eq.(24) for an arbitrary spin- n particle with n being an integer number and apply Eq.(24) to the χ_{c1} and χ_{c2} . Moreover, in order to illustrate the application of our formulas, we calculate the χ_{c1} and χ_{c2} polarizations in HX, the Collins-Soper, the Gottfried-Jackson, and the target frames at the LHC.

Note added: While this paper was prepared, a new preprint [46] for polarizations of the prompt J/ψ and ψ' production at the LHC and Tevatron appeared. The authors extracted another set of CO LDMEs for the J/ψ other than those in Refs.[18, 19] by including the χ_{cJ} and ψ' feed-down contributions. Their LDMEs result in two combinations of LDMEs that agree with that extracted in Refs.[13, 19] and their prompt polarization result is around the upper limit in Fig.2 of this paper.

⁶ Note, in the second scenario, the expressions are exactly the same as those for the J/ψ angular distribution with only E1 transition is considered as shown in Eqs.(7,11,17). Hence, the polarization observables defined in Eq.(17) have been shown in Figs.(9,12,10,13,11,14).

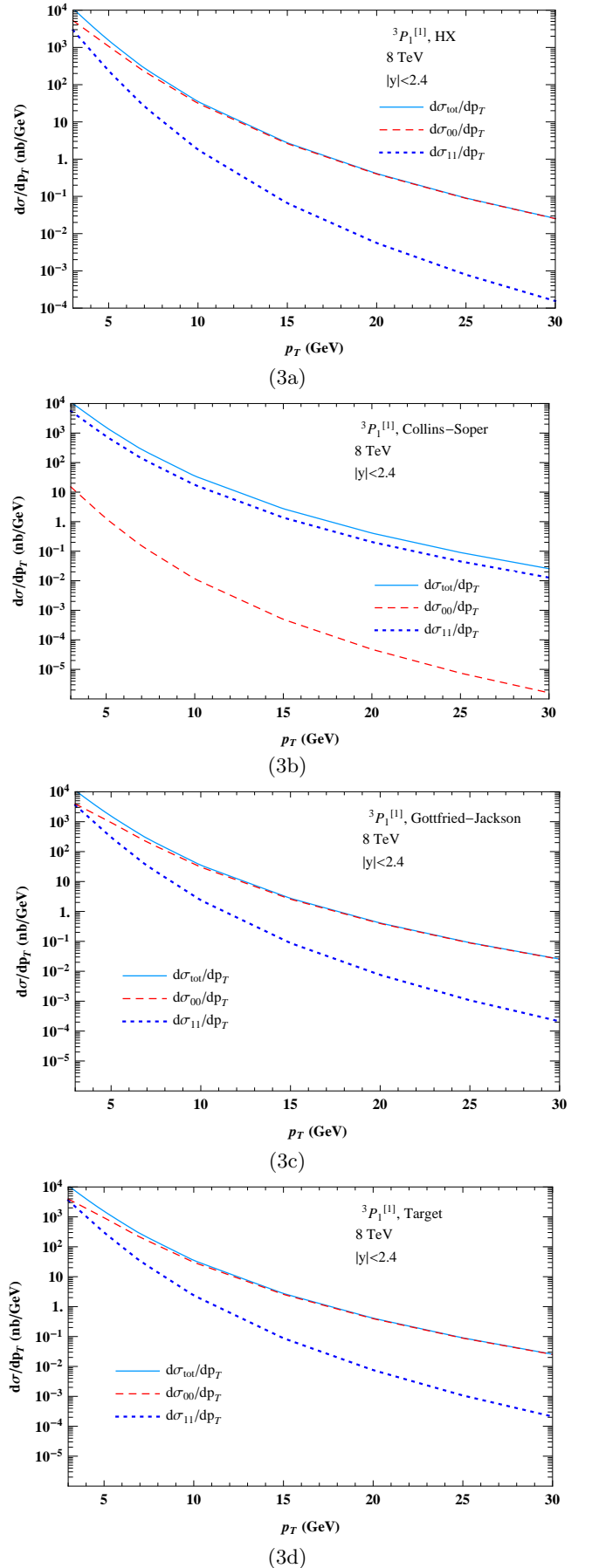
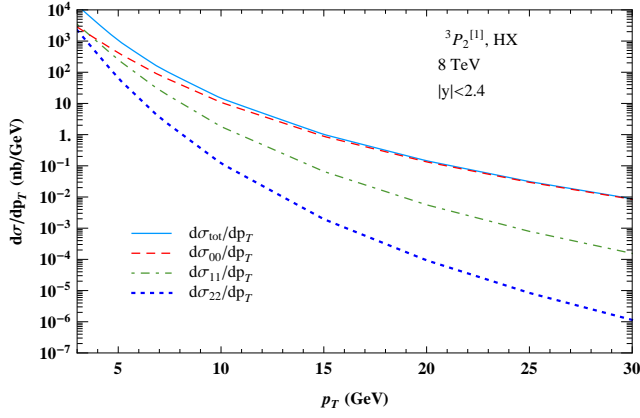
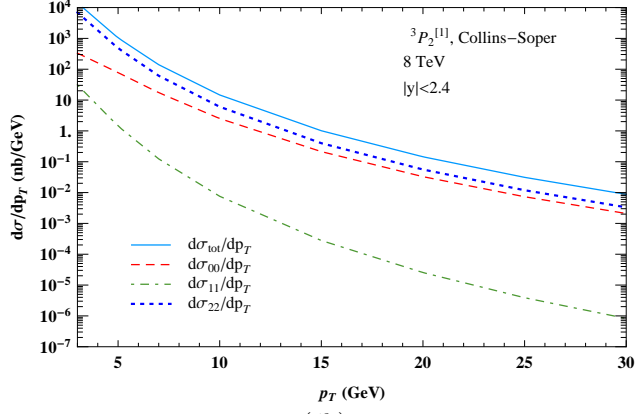


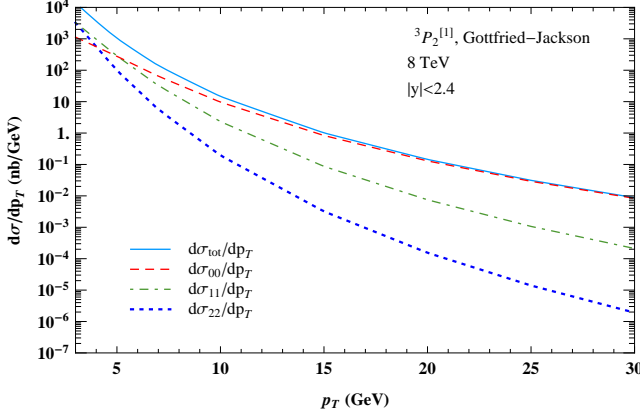
FIG. 3: Distributions of $\frac{d\sigma_{00}}{dp_T}$, $\frac{d\sigma_{11}}{dp_T}$ and $\frac{d\sigma_{tot}}{dp_T} = 2\frac{d\sigma_{11}}{dp_T} + \frac{d\sigma_{00}}{dp_T}$ for $^3P_1^{[1]}$ in HX, the Collins-Soper, the Gottfried-Jackson and the target frames.



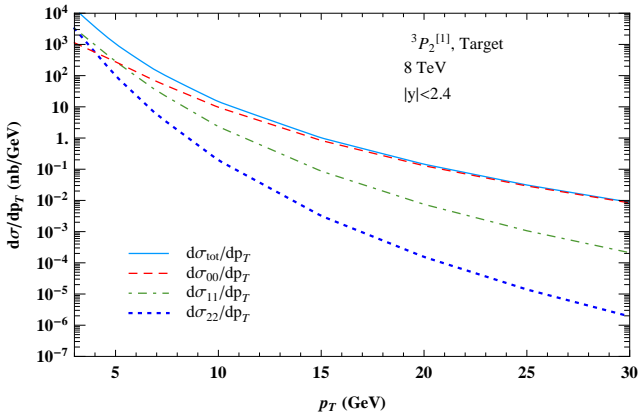
(4a)



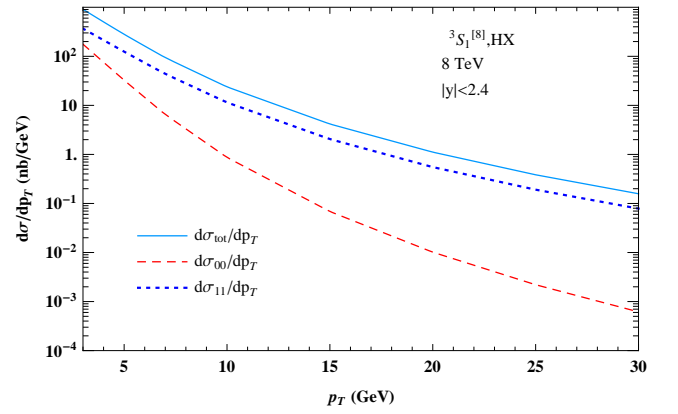
(4b)



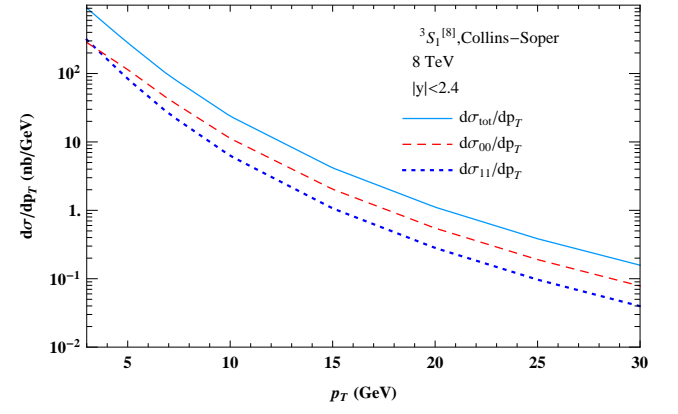
(4c)



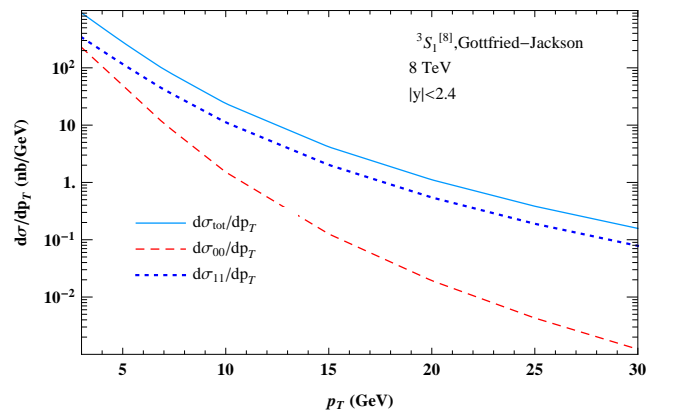
(4d)



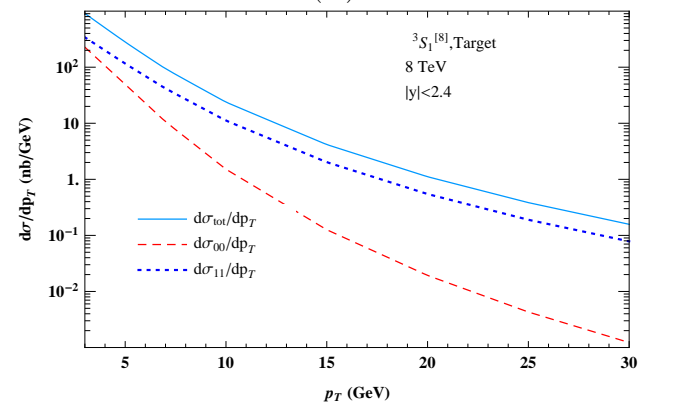
(5a)



(5b)



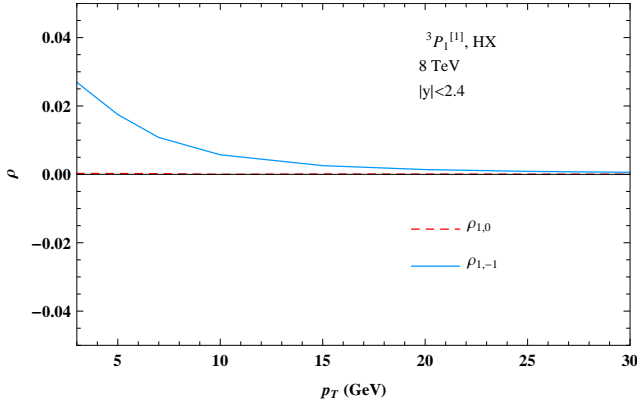
(5c)



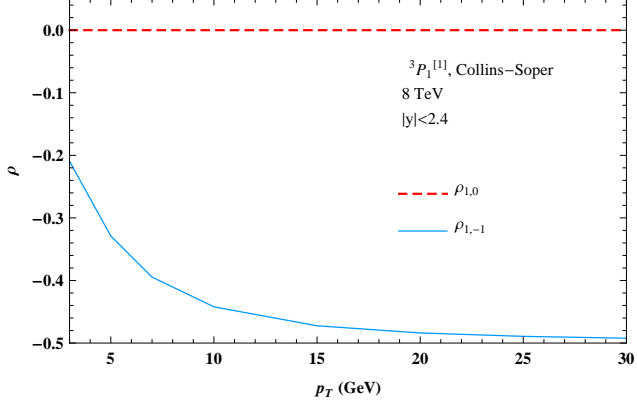
(5d)

FIG. 4: Distributions of $\frac{d\sigma_{00}}{dp_T}$, $\frac{d\sigma_{11}}{dp_T}$, $\frac{d\sigma_{22}}{dp_T}$ and $\frac{d\sigma_{tot}}{dp_T} = 2\frac{d\sigma_{22}}{dp_T} + 2\frac{d\sigma_{11}}{dp_T} + \frac{d\sigma_{00}}{dp_T}$ for $^3P_2^{[11]}$ in HX, the Collins-Soper, the Gottfried-Jackson and the target frames.

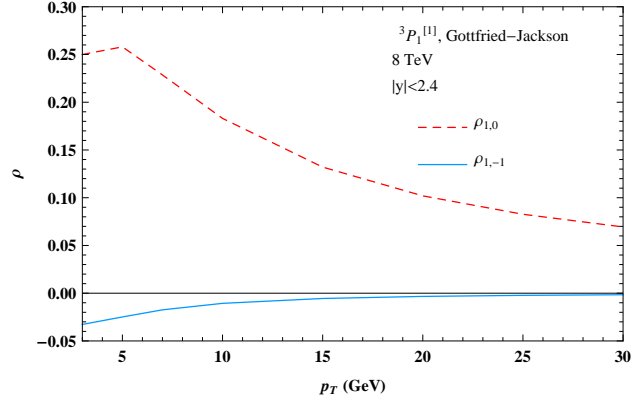
FIG. 5: Distributions of $\frac{d\sigma_{00}}{dp_T}$, $\frac{d\sigma_{11}}{dp_T}$ and $\frac{d\sigma_{tot}}{dp_T} = 2\frac{d\sigma_{11}}{dp_T} + \frac{d\sigma_{00}}{dp_T}$ for $^3S_1^{[81]}$ with $\langle\mathcal{O}^{xc0}(^3S_1^{[81]})\rangle$ used in HX, the Collins-Soper, the Gottfried-Jackson and the target frames.



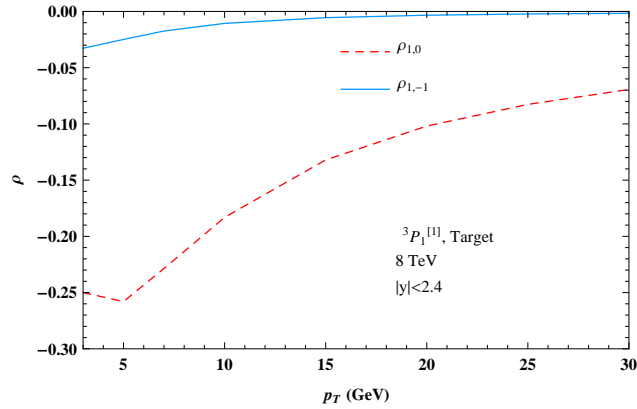
(6a)



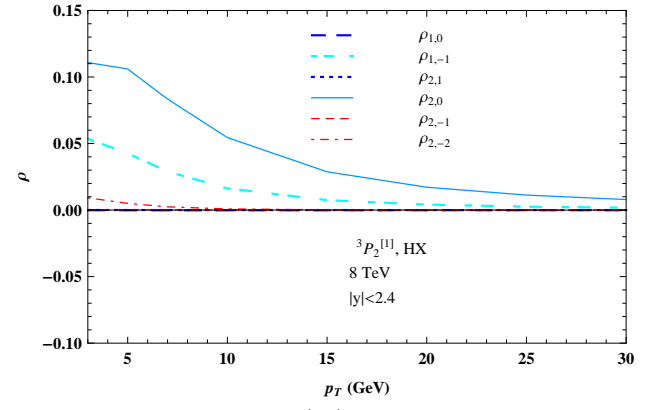
(6b)



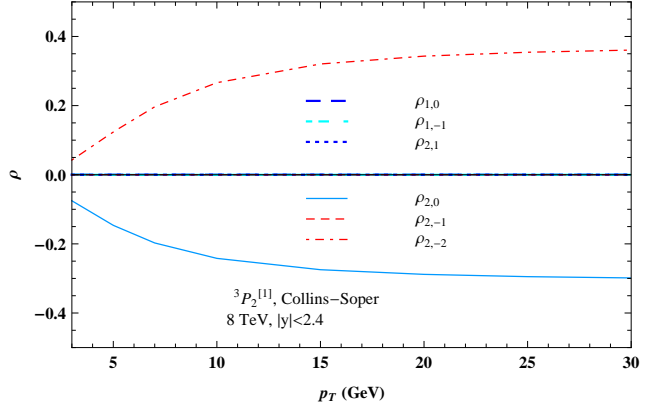
(6c)



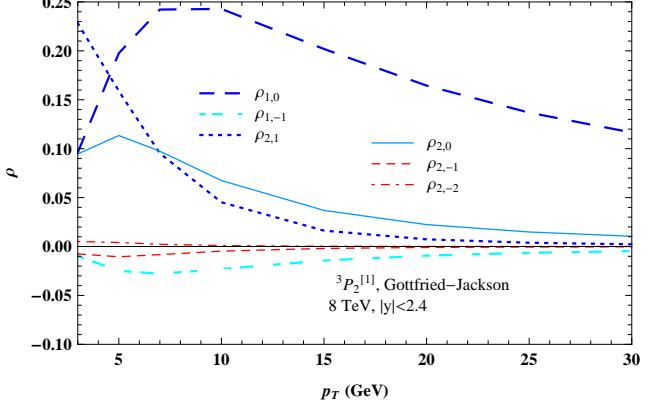
(6d)



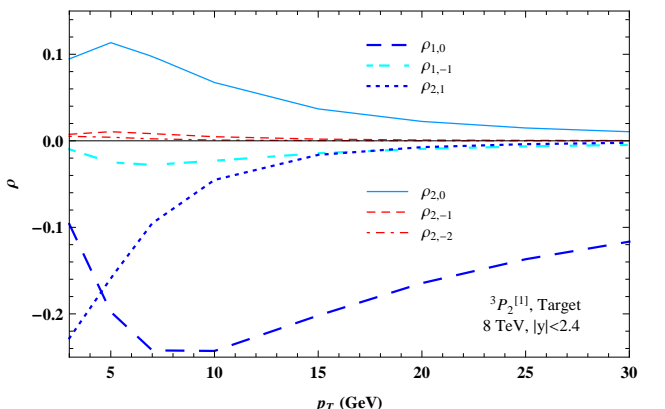
(7a)



(7b)



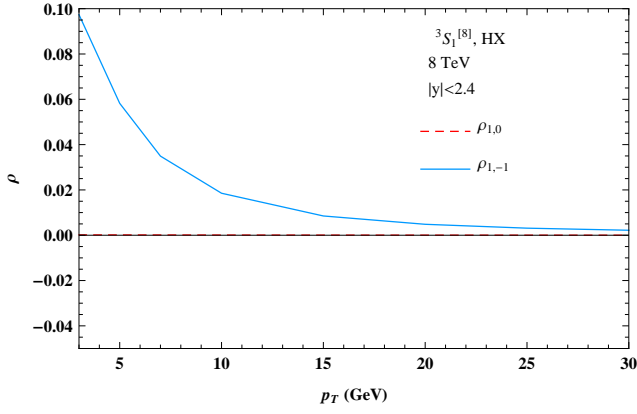
(7c)



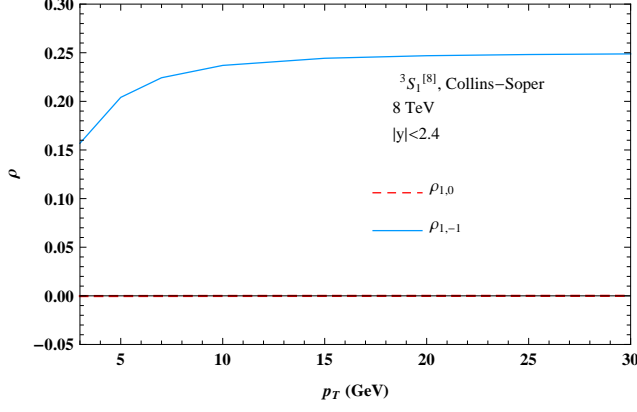
(7d)

FIG. 6: Real parts of the non-diagonal SDMEs (after normalization of $\frac{d\sigma_{\text{tot}}}{dp_T} = 2\frac{d\sigma_{11}}{dp_T} + \frac{d\sigma_{00}}{dp_T}$) for $^3P_1^{[11]}$ in the four frames.

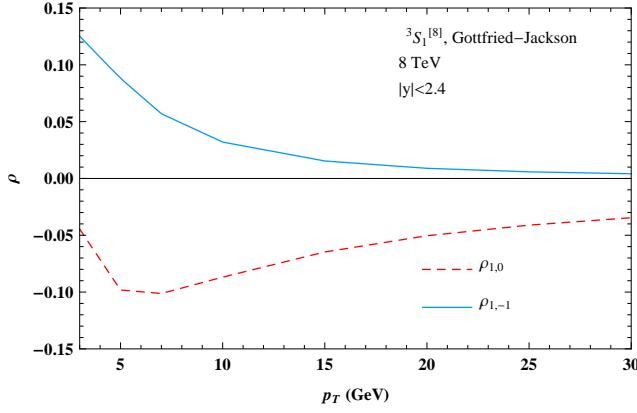
FIG. 7: Real parts of the non-diagonal SDMEs (after normalization of $\frac{d\sigma_{\text{tot}}}{dp_T} = 2\frac{d\sigma_{22}}{dp_T} + 2\frac{d\sigma_{11}}{dp_T} + \frac{d\sigma_{00}}{dp_T}$) for $^3P_2^{[11]}$ in the four frames.



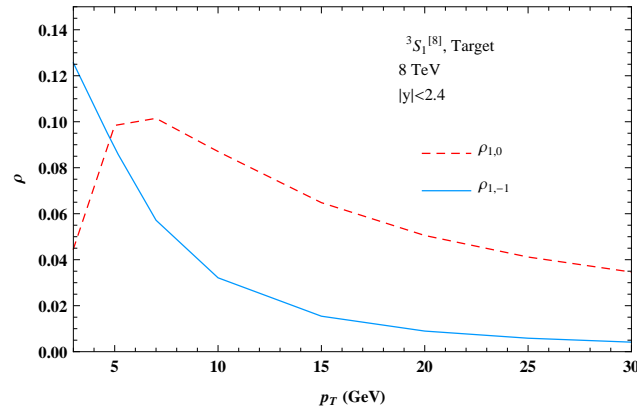
(8a)



(8b)

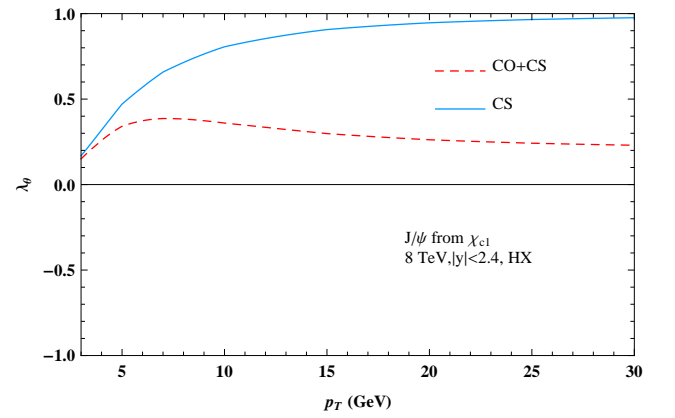


(8c)

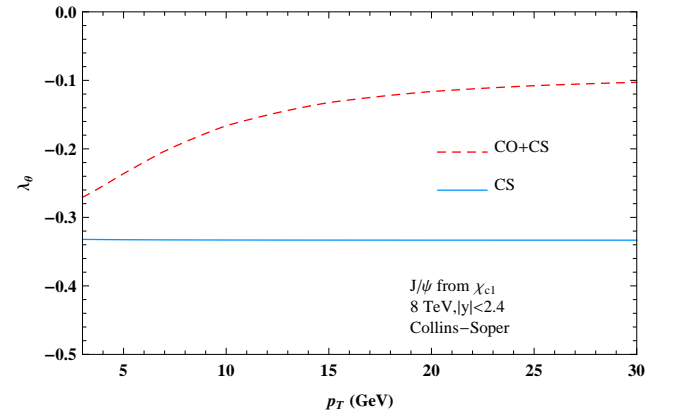


(8d)

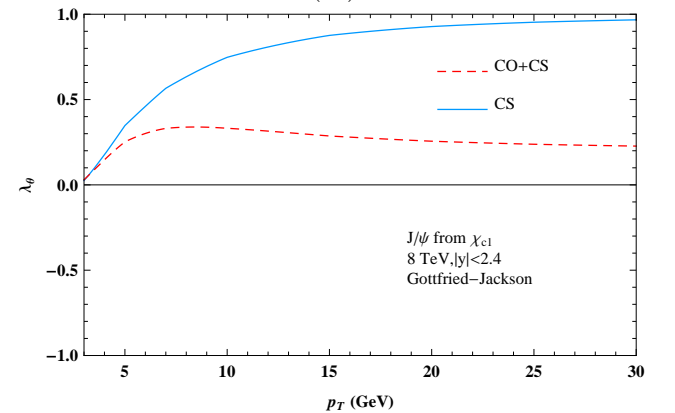
FIG. 8: Real parts of the non-diagonal SDMEs (after normalization of $\frac{d\sigma_{\text{tot}}}{dp_T} = 2\frac{d\sigma_{11}}{dp_T} + \frac{d\sigma_{00}}{dp_T}$) for ${}^3S_1^{[8]}$ in the four frames.



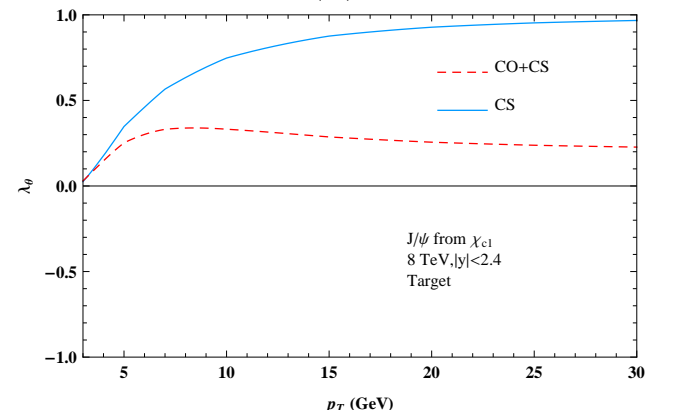
(9a)



(9b)

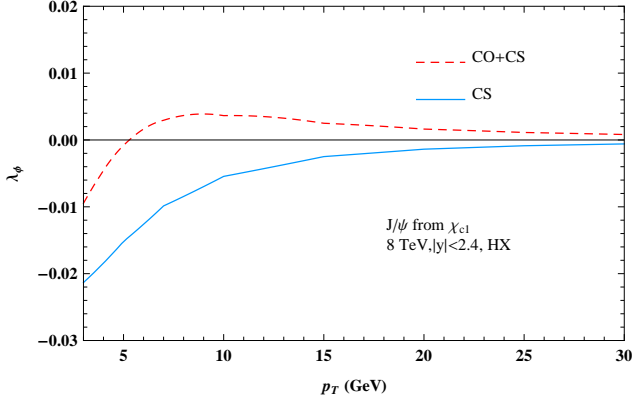


(9c)

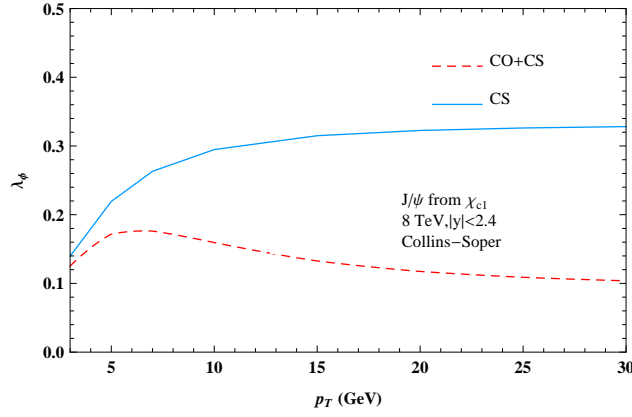


(9d)

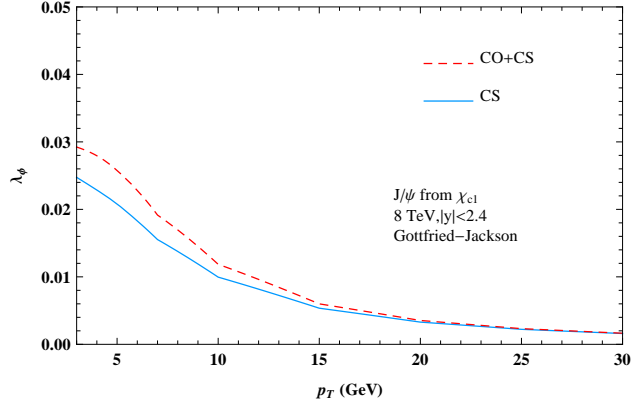
FIG. 9: Transverse momentum distribution of λ_θ describing the J/ψ angular distribution from $\chi_{c1} \rightarrow J/\psi\gamma$ in the four frames.



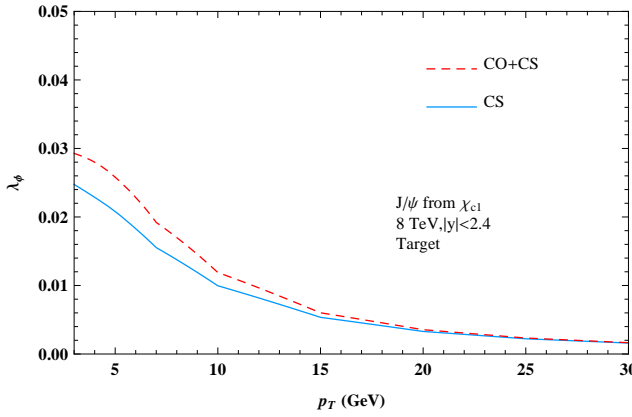
(10a)



(10b)

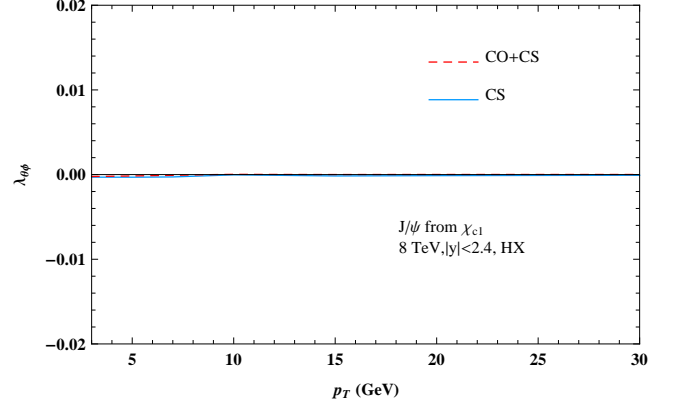


(10c)

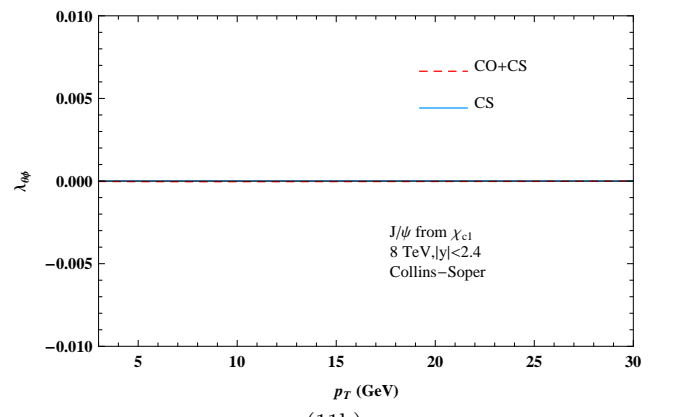


(10d)

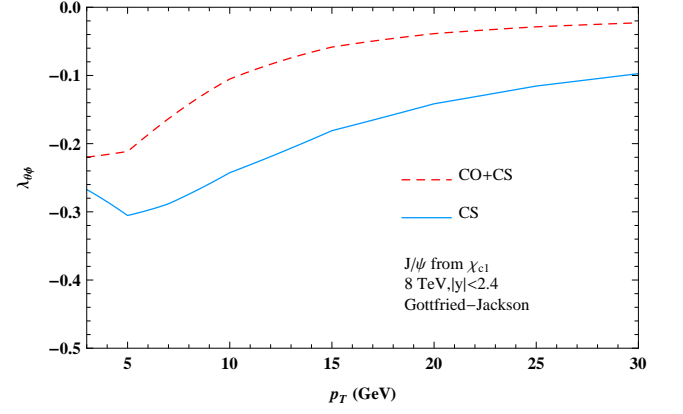
FIG. 10: Transverse momentum distribution of λ_ϕ describing the J/ψ angular distribution from $\chi_{c1} \rightarrow J/\psi\gamma$ in the four frames.



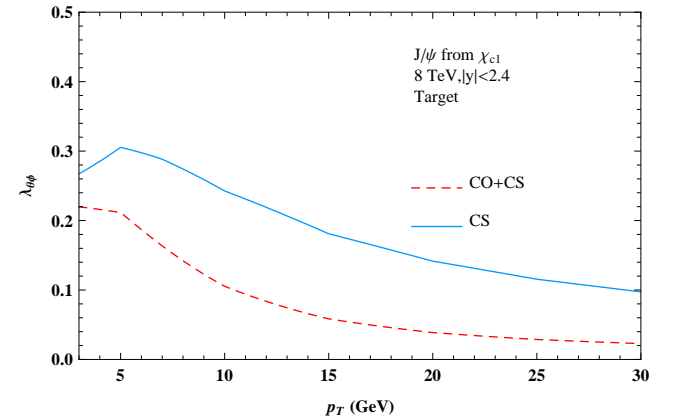
(11a)



(11b)



(11c)



(11d)

FIG. 11: Transverse momentum distribution of $\lambda_{\theta\phi}$ describing the J/ψ angular distribution from $\chi_{c1} \rightarrow J/\psi\gamma$ in the four frames.

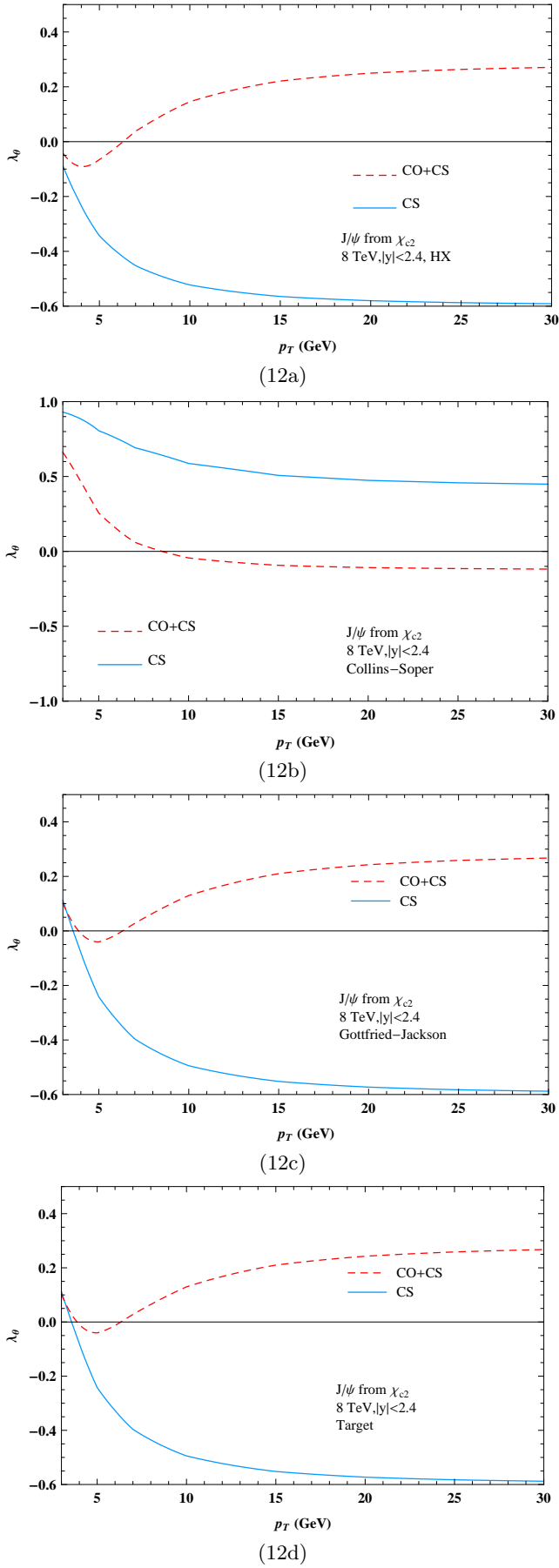


FIG. 12: Transverse momentum distribution of λ_θ describing the J/ψ angular distribution from $\chi_{c2} \rightarrow J/\psi\gamma$ in the four frames.

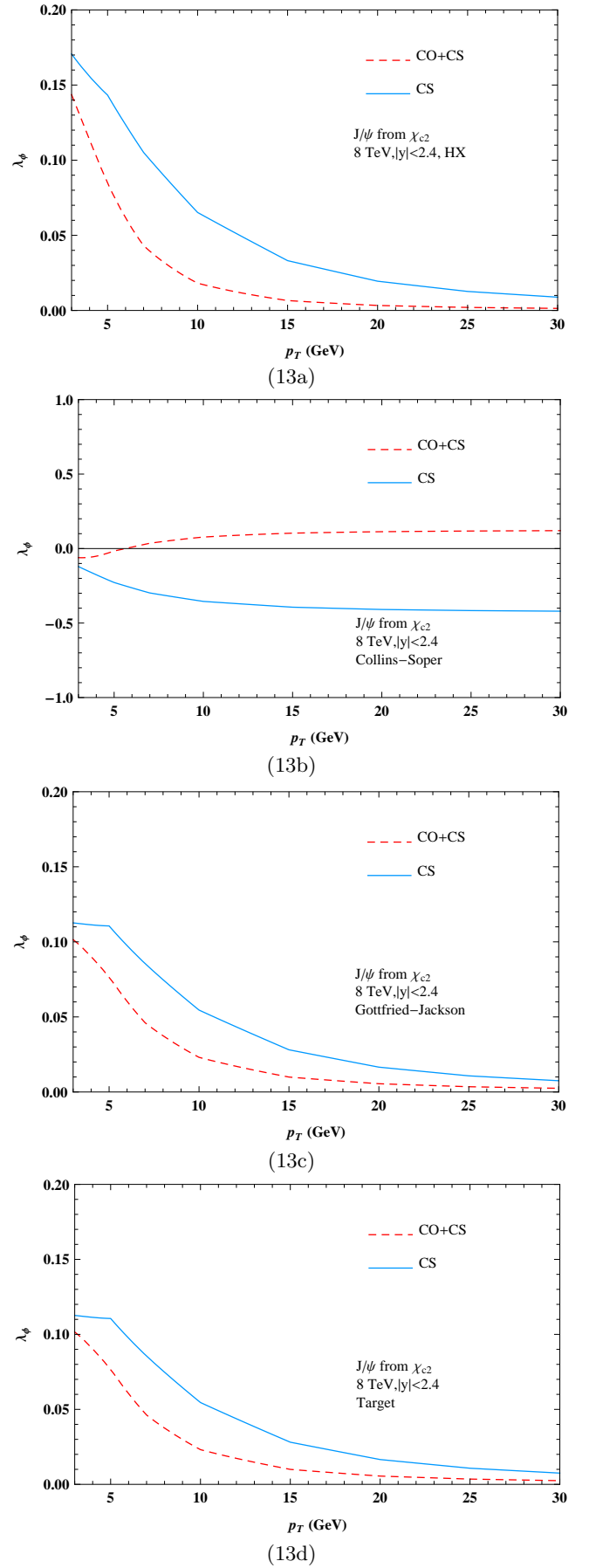
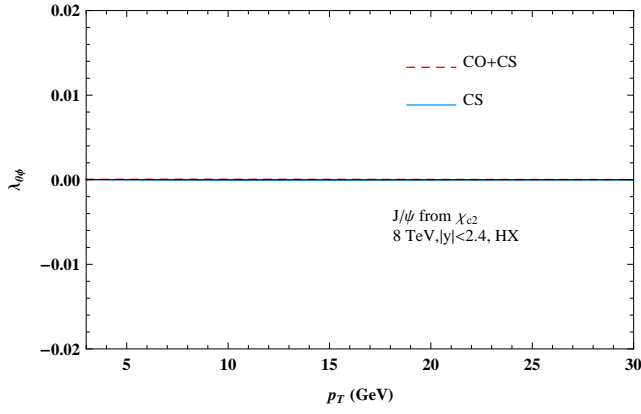
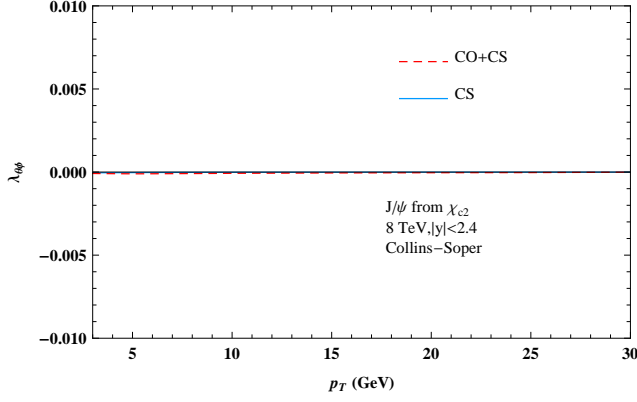


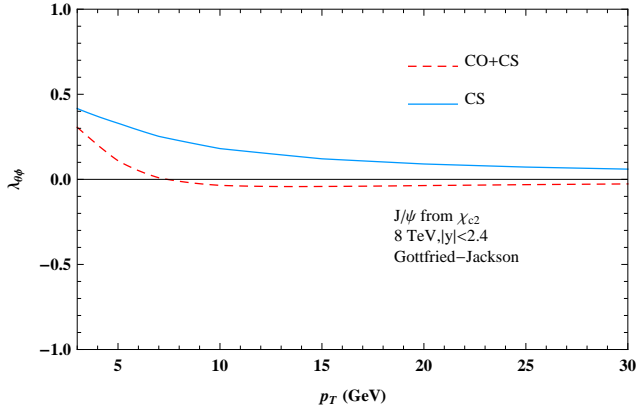
FIG. 13: Transverse momentum distribution of λ_ϕ describing the J/ψ angular distribution from $\chi_{c2} \rightarrow J/\psi\gamma$ in the four frames.



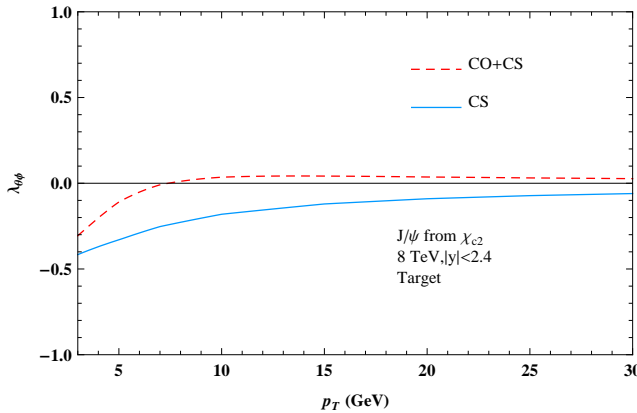
(14a)



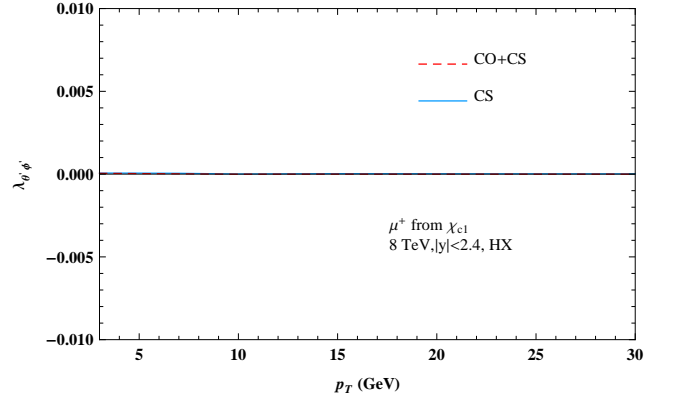
(14b)



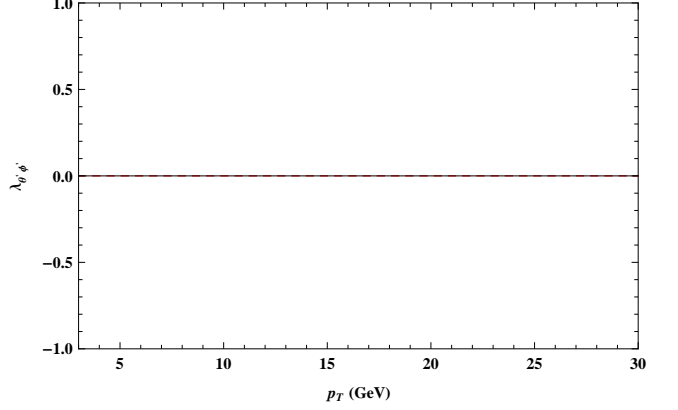
(14c)



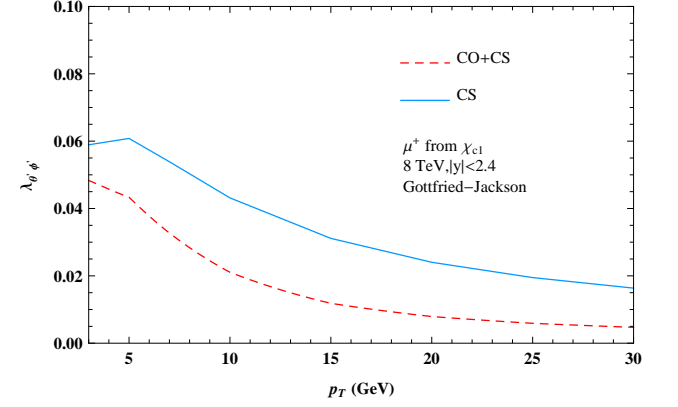
(14d)



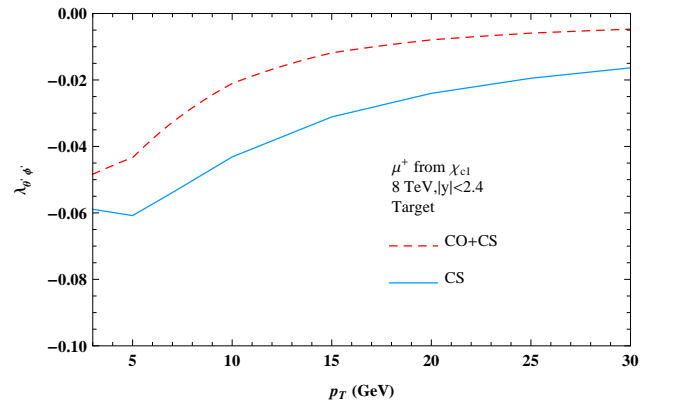
(15a)



(15b)



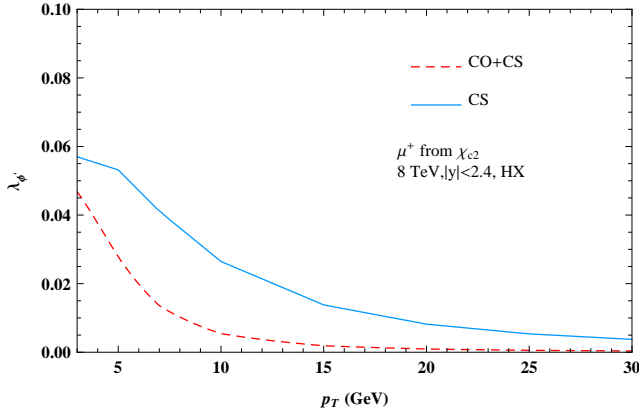
(15c)



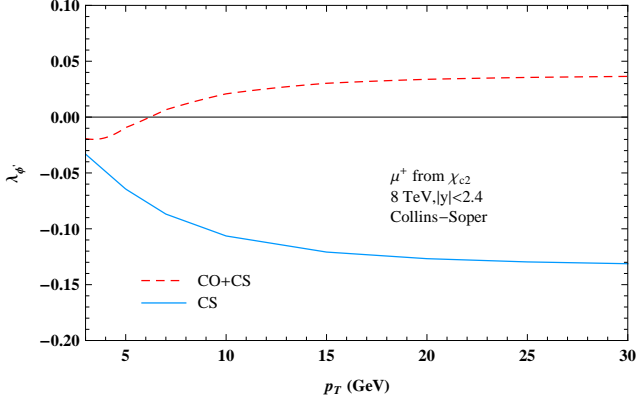
(15d)

FIG. 14: Transverse momentum distribution of $\lambda_{\theta\phi}$ describing the J/ψ angular distribution from $\chi_{c2} \rightarrow J/\psi\gamma$ in the four frames.

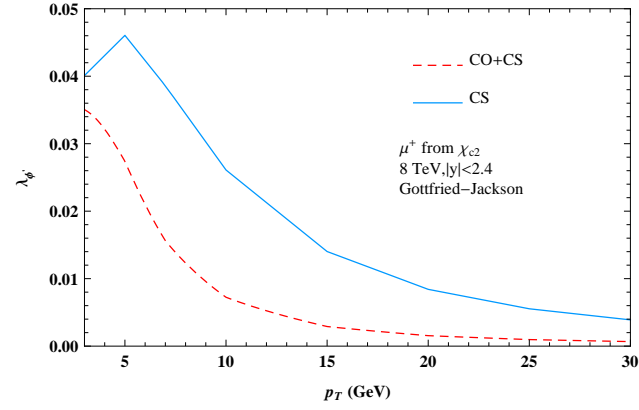
FIG. 15: Transverse momentum distribution of $\lambda_{\theta'\phi'}$ describing the μ^+ angular distribution from cascade decay $\chi_{c1} \rightarrow J/\psi\gamma \rightarrow \mu^+\mu^-\gamma$ in the first scenario.



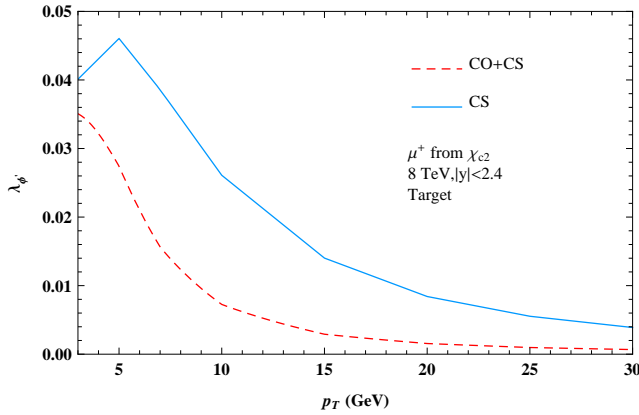
(16a)



(16b)

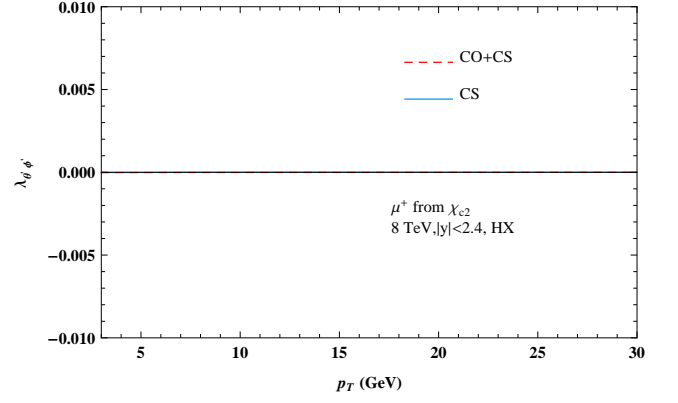


(16c)

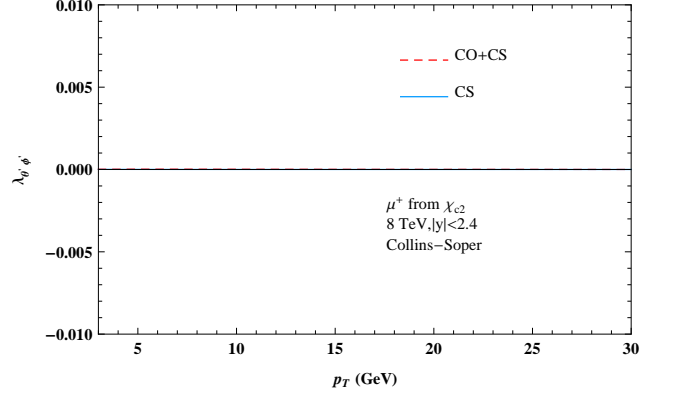


(16d)

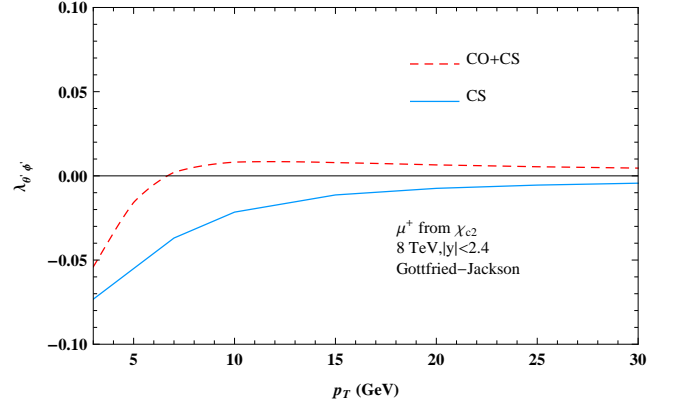
FIG. 16: Transverse momentum distribution of $\lambda_{\phi'}$ describing the μ^+ angular distribution from cascade decay $\chi_{c2} \rightarrow J/\psi \gamma \rightarrow \mu^+ \mu^- \gamma$ in the first scenario.



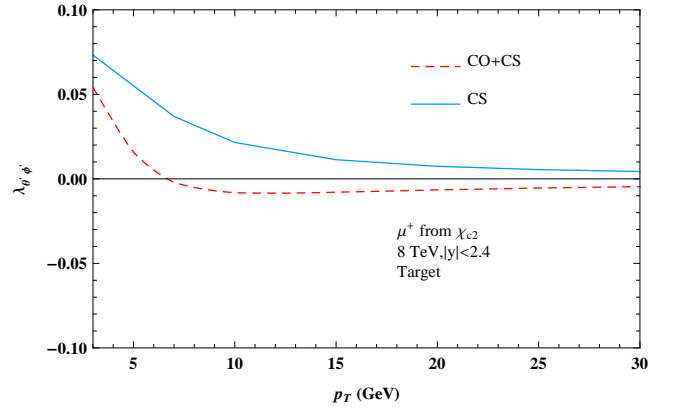
(17a)



(17b)

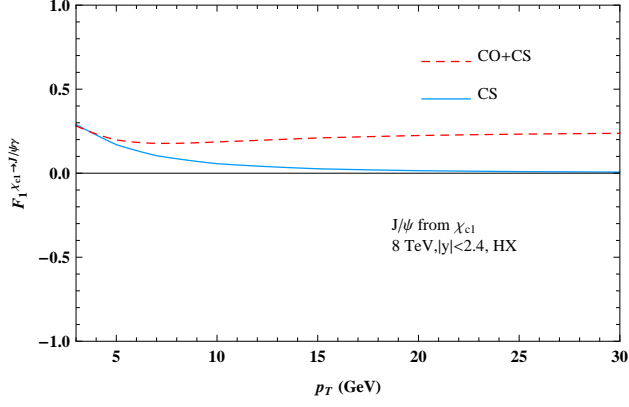


(17c)

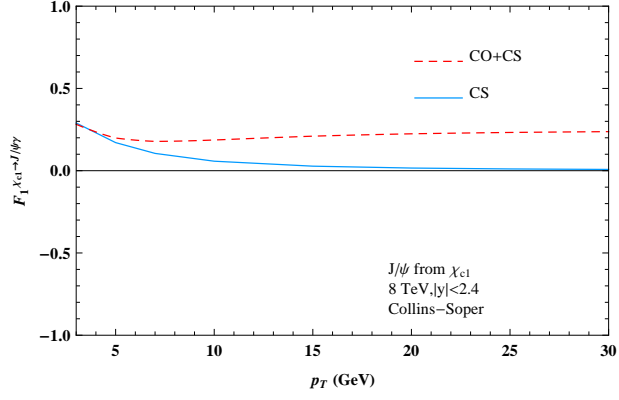


(17d)

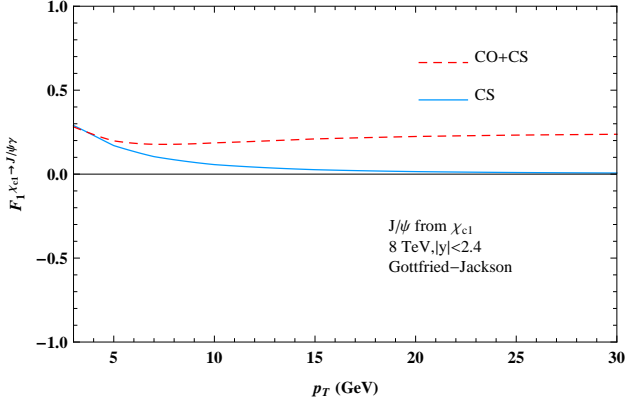
FIG. 17: Transverse momentum distribution of $\lambda_{\theta' \phi'}$ that describing the μ^+ angular distribution from cascade decay $\chi_{c2} \rightarrow J/\psi \gamma \rightarrow \mu^+ \mu^- \gamma$ in the first scenario.



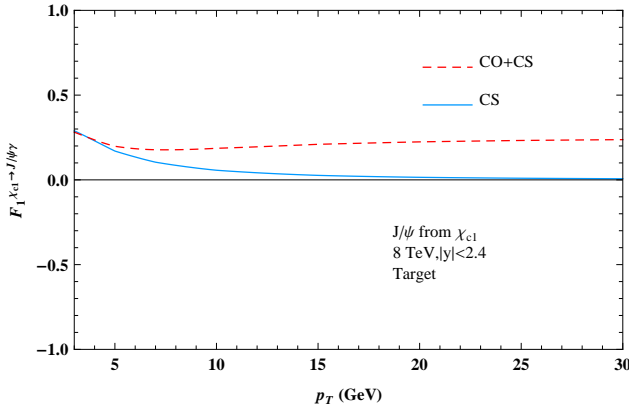
(18a)



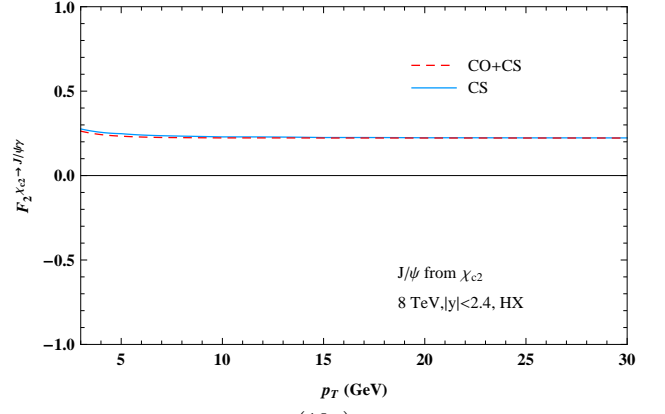
(18b)



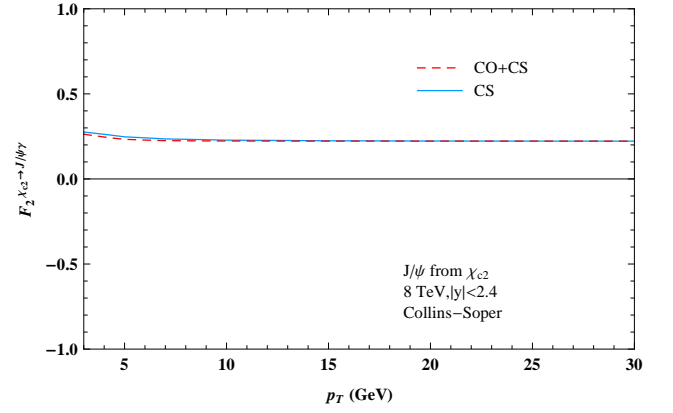
(18c)



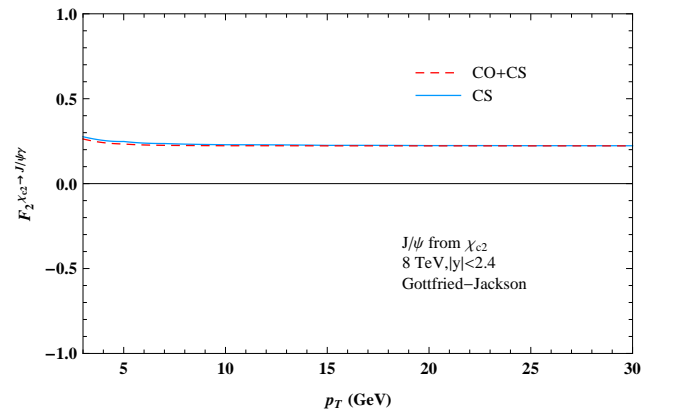
(18d)



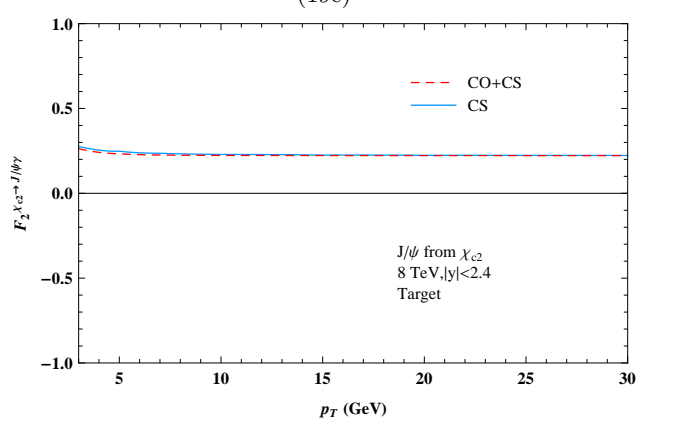
(19a)



(19b)



(19c)



(19d)

FIG. 18: Transverse momentum distribution of $F_1^{\chi_{c1} \rightarrow J/\psi\gamma}$ defined in Eq.(25), which shows that $F_1^{\chi_{c1} \rightarrow J/\psi\gamma}$ is frame-independent.

FIG. 19: Transverse momentum distribution of $F_2^{\chi_{c2} \rightarrow J/\psi\gamma}$ defined in Eq.(26), which shows that $F_2^{\chi_{c2} \rightarrow J/\psi\gamma}$ is frame-independent.

Acknowledgments

We thank J.P. Lansberg, Q.H. Cao and Y.Q. Ma for helpful discussions. This work was supported in part by the National Natural Science Foundation of China (Nos.11021092,11075002), and the Ministry of Science and Technology of China (No.2009CB825200).

Appendix A: Angular distributions in the spin-1 boson decay

In the appendix, we list the general angular distribution of the decay products from a vector boson V without any symmetry assumptions as

$$\begin{aligned} \mathcal{W}^V(\theta, \phi) \propto & 1 + \lambda_\theta \cos^2 \theta + \lambda_\phi \sin^2 \theta \cos \phi \\ & + \lambda_{\theta\phi} \sin 2\theta \cos \phi + \lambda_\phi^\perp \sin^2 \theta \sin 2\phi \\ & + \lambda_{\phi\phi}^\perp \sin 2\theta \sin \phi + 2\eta_\theta \cos \theta \\ & + 2\eta_{\theta\phi} \sin \theta \cos \phi + 2\eta_{\theta\phi}^\perp \sin \theta \sin \phi, \quad (\text{A1}) \end{aligned}$$

with

$$\begin{aligned} \lambda_\theta &= (1-3\delta) \frac{N_V - 3\rho_{0,0}^V}{(1+\delta)N_V + (1-3\delta)\rho_{0,0}^V}, \\ \lambda_\phi &= (1-3\delta) \frac{2\Re\rho_{1,-1}^V}{(1+\delta)N_V + (1-3\delta)\rho_{0,0}^V}, \\ \lambda_{\theta\phi} &= (1-3\delta) \frac{\sqrt{2}(\Re\rho_{1,0}^V - \Re\rho_{-1,0}^V)}{(1+\delta)N_V + (1-3\delta)\rho_{0,0}^V}, \\ \lambda_\phi^\perp &= -(1-3\delta) \frac{2\Im\rho_{1,-1}^V}{(1+\delta)N_V + (1-3\delta)\rho_{0,0}^V}, \\ \lambda_{\theta\phi}^\perp &= -(1-3\delta) \frac{\sqrt{2}(\Im\rho_{1,0}^V + \Im\rho_{-1,0}^V)}{(1+\delta)N_V + (1-3\delta)\rho_{0,0}^V}, \\ \eta_\theta &= \alpha \frac{\rho_{1,1}^V - \rho_{-1,-1}^V}{(1+\delta)N_V + (1-3\delta)\rho_{0,0}^V}, \\ \eta_{\theta\phi} &= \alpha \frac{\sqrt{2}(\Re\rho_{1,0}^V + \Re\rho_{-1,0}^V)}{(1+\delta)N_V + (1-3\delta)\rho_{0,0}^V}, \\ \eta_{\theta\phi}^\perp &= -\alpha \frac{\sqrt{2}(\Im\rho_{1,0}^V - \Im\rho_{-1,0}^V)}{(1+\delta)N_V + (1-3\delta)\rho_{0,0}^V}, \quad (\text{A2}) \end{aligned}$$

where $N_V = \rho_{1,1}^V + \rho_{0,0}^V + \rho_{-1,-1}^V$, and parameters α, δ are specified by the identifications of V and its decay products. In particular, α is induced by the parity violating interactions in the decay. In other words, it is non-zero only when the decay is not a parity conservative process. For the J/ψ decays into di-lepton, $\alpha = 0, \delta = 0$, while for the pure E1 radiative transition $\chi_{c1} \rightarrow J/\psi\gamma, \alpha = 0, \delta = \frac{1}{2}$. If one also wants to include the M2 transition in the χ_{c1} decay, δ should be changed to $\frac{1+2a_1^{J=1}a_2^{J=1}}{2}$, where $a_1^{J=1}, a_2^{J=1}$ represent the E1 and M2 amplitudes with the normalization $(a_1^{J=1})^2 + (a_2^{J=1})^2 = 1$ respectively. Their

values have been measured in Refs.[26, 27, 29]. The numerical values measured are shown in TabII. Without losing generalities, the rotation-invariant observable F_1 defined in Eq.(25) can be written as

$$F_1 = \frac{1 - 3\delta + (1 - \delta)\lambda_\theta + 2\lambda_\phi}{(1 - 3\delta)(3 + \lambda_\theta)}. \quad (\text{A3})$$

Experiment	$a_2^{J=1}(10^{-2})$
CLEO[26]	$-6.26 \pm 0.63 \pm 0.24$
Crystal Ball [27]	$-0.2^{+0.8}_{-2.0}$
E835 [29]	$0.2 \pm 3.2 \pm 0.4$

TABLE II: The M2 normalized amplitude $a_2^{J=1}$ for $\chi_{c1} \rightarrow J/\psi\gamma$ measured by different experiments.

Appendix B: Angular distributions in the spin-2 boson decay

For the spin-2 tensor particles, the relevant angular distributions are more complicated than that in the previous appendix. Here we neglect the details, and only write down the angular distribution for a spin-2 tensor particle T_2 decay in a general form:

$$\begin{aligned} \mathcal{W}^{T_2}(\theta, \phi) \propto & 1 + \lambda_\theta \cos^2 \theta + \lambda_{2\theta} \cos^4 \theta \\ & + \lambda_{\theta\phi} \sin 2\theta \cos \phi + \lambda_{2\theta\phi} \sin 2\theta \sin^2 \theta \cos \phi \\ & + \lambda_{\theta\phi}^\perp \sin 2\theta \sin \phi + \lambda_{2\theta\phi}^\perp \sin 2\theta \sin^2 \theta \sin \phi \\ & + \lambda_\phi \sin^2 \theta \cos 2\phi + \lambda_{2\phi} \sin^4 \theta \cos 2\phi \\ & + \lambda_\phi^\perp \sin^2 \theta \sin 2\phi + \lambda_{2\phi}^\perp \sin^4 \theta \sin 2\phi \\ & + \lambda_{3\theta\phi} \sin 2\theta \sin^2 \theta \cos 3\phi \\ & + \lambda_{3\theta\phi}^\perp \sin 2\theta \sin^2 \theta \sin 3\phi \\ & + \lambda_{4\phi} \sin^4 \theta \cos 4\phi + \lambda_{4\phi}^\perp \sin^4 \theta \sin 4\phi \\ & + 2\eta_\theta \cos \theta + 2\eta_{2\theta} \cos^3 \theta \\ & + 2\eta_{\theta\phi} \sin \theta \cos \phi + 2\eta_{2\theta\phi} \sin^3 \theta \cos \phi \\ & + 2\eta_{\theta\phi}^\perp \sin \theta \sin \phi + 2\eta_{2\theta\phi}^\perp \sin^3 \theta \sin \phi \\ & + 2\eta_\phi \sin^2 \theta \cos \theta \cos 2\phi + 2\eta_\phi^\perp \sin^2 \theta \cos \theta \sin 2\phi \\ & + 2\eta_{3\theta\phi} \sin^3 \theta \cos 3\phi \\ & + 2\eta_{3\theta\phi}^\perp \sin^3 \theta \sin 3\phi, \quad (\text{B1}) \end{aligned}$$

where the coefficients in the above expression are

$$\begin{aligned}
\lambda_\theta &= 6[(1 - 3\delta_0 - \delta_1)N_{T_2} \\
&\quad - (1 - 7\delta_0 + \delta_1)(\rho_{1,1}^{T_2} + \rho_{-1,-1}^{T_2}) \\
&\quad - (3 - \delta_0 - 7\delta_1)\rho_{0,0}^{T_2}]/R, \\
\lambda_{2\theta} &= (1 + 5\delta_0 - 5\delta_1)[N_{T_2} - 5(\rho_{1,1}^{T_2} + \rho_{-1,-1}^{T_2}) \\
&\quad + 5\rho_{0,0}^{T_2}]/R, \\
\lambda_{\theta\phi} &= 4[2(1 - \delta_0 - 2\delta_1)(\Re\rho_{2,1}^{T_2} - \Re\rho_{-2,-1}^{T_2}) \\
&\quad - \sqrt{6}(2\delta_0 - \delta_1)(\Re\rho_{1,0}^{T_2} - \Re\rho_{-1,0}^{T_2})]/R, \\
\lambda_{2\theta\phi} &= -2(1 + 5\delta_0 - 5\delta_1)[(\Re\rho_{2,1}^{T_2} - \Re\rho_{-2,-1}^{T_2}) \\
&\quad - \sqrt{6}(\Re\rho_{1,0}^{T_2} - \Re\rho_{-1,0}^{T_2})]/R, \\
\lambda_{\theta\phi}^\perp &= 4[-2(1 - \delta_0 - 2\delta_1)(\Im\rho_{2,1}^{T_2} + \Im\rho_{-2,-1}^{T_2}) \\
&\quad + \sqrt{6}(2\delta_0 - \delta_1)(\Im\rho_{1,0}^{T_2} + \Im\rho_{-1,0}^{T_2})]/R, \\
\lambda_{2\theta\phi}^\perp &= 2(1 + 5\delta_0 - 5\delta_1)[(\Im\rho_{2,1}^{T_2} + \Im\rho_{-2,-1}^{T_2}) \\
&\quad - \sqrt{6}(\Im\rho_{1,0}^{T_2} + \Im\rho_{-1,0}^{T_2})]/R, \\
\lambda_\phi &= 4[\sqrt{6}(1 + \delta_0 - 3\delta_1)(\Re\rho_{2,0}^{T_2} + \Re\rho_{-2,0}^{T_2}) \\
&\quad - 6(2\delta_0 - \delta_1)\Re\rho_{1,-1}^{T_2}]/R, \\
\lambda_{2\phi} &= -2(1 + 5\delta_0 - 5\delta_1)[\sqrt{6}(\Re\rho_{2,0}^{T_2} + \Re\rho_{-2,0}^{T_2}) \\
&\quad - 4\Re\rho_{1,-1}^{T_2}]/R, \\
\lambda_\phi^\perp &= -4[\sqrt{6}(1 + \delta_0 - 3\delta_1)(\Im\rho_{2,0}^{T_2} - \Im\rho_{-2,0}^{T_2}) \\
&\quad - 6(2\delta_0 - \delta_1)\Im\rho_{1,-1}^{T_2}]/R, \\
\lambda_{2\phi}^\perp &= 2(1 + 5\delta_0 - 5\delta_1)[\sqrt{6}(\Im\rho_{2,0}^{T_2} - \Im\rho_{-2,0}^{T_2}) \\
&\quad - 4\Im\rho_{1,-1}^{T_2}]/R, \\
\lambda_{3\theta\phi} &= 2(1 + 5\delta_0 - 5\delta_1)\frac{\Re\rho_{2,-1}^{T_2} - \Re\rho_{-2,1}^{T_2}}{R}, \\
\lambda_{3\theta\phi}^\perp &= -2(1 + 5\delta_0 - 5\delta_1)\frac{\Im\rho_{2,-1}^{T_2} + \Im\rho_{-2,1}^{T_2}}{R}, \\
\lambda_{4\phi} &= 2(1 + 5\delta_0 - 5\delta_1)\frac{\Re\rho_{2,-2}^{T_2}}{R}, \\
\lambda_{4\phi}^\perp &= -2(1 + 5\delta_0 - 5\delta_1)\frac{\Im\rho_{2,-2}^{T_2}}{R},
\end{aligned} \tag{B2}$$

and

$$\begin{aligned}
\eta_\theta &= 2[(2\alpha_1 + \alpha_2)(\rho_{2,2}^{T_2} - \rho_{-2,-2}^{T_2}) \\
&\quad - 2(\alpha_1 - \alpha_2)(\rho_{1,1}^{T_2} - \rho_{-1,-1}^{T_2})]/R, \\
\eta_{2\theta} &= -2(2\alpha_1 - \alpha_2)[(\rho_{2,2}^{T_2} - \rho_{-2,-2}^{T_2}) \\
&\quad - 2(\rho_{1,1}^{T_2} - \rho_{-1,-1}^{T_2})]/R, \\
\eta_{\theta\phi} &= -4[2(\alpha_1 - \alpha_2)(\Re\rho_{2,1}^{T_2} + \Re\rho_{-2,-1}^{T_2}) \\
&\quad - \sqrt{6}\alpha_1(\Re\rho_{1,0}^{T_2} + \Re\rho_{-1,0}^{T_2})]/R, \\
\eta_{2\theta\phi} &= 2(2\alpha_1 - \alpha_2)[3(\Re\rho_{2,1}^{T_2} + \Re\rho_{-2,-1}^{T_2}) \\
&\quad - \sqrt{6}(\Re\rho_{1,0}^{T_2} + \Re\rho_{-1,0}^{T_2})]/R, \\
\eta_{\theta\phi}^\perp &= 4[2(\alpha_1 - \alpha_2)(\Im\rho_{2,1}^{T_2} - \Im\rho_{-2,-1}^{T_2}) \\
&\quad - \sqrt{6}\alpha_1(\Im\rho_{1,0}^{T_2} - \Im\rho_{-1,0}^{T_2})]/R, \\
\eta_{2\theta\phi}^\perp &= -2(2\alpha_1 - \alpha_2)[3(\Im\rho_{2,1}^{T_2} - \Im\rho_{-2,-1}^{T_2}) \\
&\quad - \sqrt{6}(\Im\rho_{1,0}^{T_2} - \Im\rho_{-1,0}^{T_2})]/R, \\
\eta_\phi &= -2\sqrt{6}(2\alpha_1 - \alpha_2)\frac{\Re\rho_{2,0}^{T_2} - \Re\rho_{-2,0}^{T_2}}{R}, \\
\eta_\phi^\perp &= 2\sqrt{6}(2\alpha_1 - \alpha_2)\frac{\Im\rho_{2,0}^{T_2} + \Im\rho_{-2,0}^{T_2}}{R}, \\
\eta_{3\theta\phi} &= -2(2\alpha_1 - \alpha_2)\frac{\Re\rho_{2,-1}^{T_2} + \Re\rho_{-2,1}^{T_2}}{R}, \\
\eta_{3\theta\phi}^\perp &= 2(2\alpha_1 - \alpha_2)\frac{\Im\rho_{2,-1}^{T_2} - \Im\rho_{-2,1}^{T_2}}{R},
\end{aligned} \tag{B3}$$

with

$$\begin{aligned}
N_{T_2} &= \rho_{2,2}^{T_2} + \rho_{1,1}^{T_2} + \rho_{0,0}^{T_2} + \rho_{-1,-1}^{T_2} + \rho_{-2,-2}^{T_2}, \\
R &= (1 + 5\delta_0 + 3\delta_1)N_{T_2} \\
&\quad + 3(1 - 3\delta_0 - \delta_1)(\rho_{1,1}^{T_2} + \rho_{-1,-1}^{T_2}) \\
&\quad + (5 - 7\delta_0 - 9\delta_1)\rho_{0,0}^{T_2}.
\end{aligned} \tag{B4}$$

In analogy, the parameters α_1 and α_2 are vanishing when parity is not violated. In other words, these coefficients exhibited in Eq.(B3) are zero in the case of the χ_{c2} decay. Other two parameters, δ_0 and δ_1 , can be determined from the specific processes one considered. For the χ_{c2} decays into a J/ψ and a photon, through pure E1 transition, $\delta_0 = \frac{1}{10}$ and $\delta_1 = \frac{3}{10}$, while after including the higher-order multipole amplitudes in the radiative transitions, the coefficients δ_0 and δ_1 can be expressed as the polynomial of E1, M2 and E3 amplitudes $a_1^{J=2}, a_2^{J=2}, a_3^{J=2}$

$$\begin{aligned}
\delta_0 &= [1 + 2a_1^{J=2}(\sqrt{5}a_2^{J=2} + 2a_3^{J=2}) \\
&\quad + 4a_2^{J=2}(a_2^{J=2} + \sqrt{5}a_3^{J=2}) + 3(a_3^{J=2})^2]/10, \\
\delta_1 &= [9 + 6a_1^{J=2}(\sqrt{5}a_2^{J=2} - 4a_3^{J=2}) \\
&\quad - 4a_2^{J=2}(a_2^{J=2} + 2\sqrt{5}a_3^{J=2}) + 7(a_3^{J=2})^2]/30.
\end{aligned} \tag{B5}$$

Again, the normalization of $(a_1^{J=2})^2 + (a_2^{J=2})^2 + (a_3^{J=2})^2 = 1$ has been implicitly understood. The numerical values extracted from the experiments can also be found in

Refs.[26–29] and we summarize them in Tab.III. At last, we denote F_2 in terms of the coefficients in Eq.(B1):

$$\begin{aligned}
F_2 &= \frac{n_1 + n_2\lambda_\theta + n_3\lambda_{2\theta} + n_4\lambda_\phi + n_5\lambda_{2\phi} + n_6\lambda_{4\phi}}{d_1 + d_2\lambda_\theta + d_3\lambda_{2\theta}}, \\
n_1 &= \frac{1}{6}, \\
n_2 &= \frac{4 - 4\delta_0 - 3\delta_1}{18(2 - 4\delta_0 - 3\delta_1)}, \\
n_3 &= \frac{2 + 2\delta_0 - 7\delta_1 - 4\delta_0^2 + \delta_0\delta_1 + 3\delta_1^2}{6(1 + 5\delta_0 - 5\delta_1)(2 - 4\delta_0 - 3\delta_1)}, \\
n_4 &= \frac{1}{3(2 - 4\delta_0 - 3\delta_1)}, \\
n_5 &= \frac{2\delta_0 - \delta_1}{(1 + 5\delta_0 - 5\delta_1)(2 - 4\delta_0 - 3\delta_1)}, \\
n_6 &= \frac{1}{1 + 5\delta_0 - 5\delta_1}, \\
d_1 &= \frac{15}{16}, d_2 = \frac{5}{16}, d_3 = \frac{3}{16}.
\end{aligned} \tag{B6}$$

Experiment	$a_2^{J=2}(10^{-2})$	$a_3^{J=2}(10^{-2})$
CLEO(Fit 1)[26]	$-9.3 \pm 1.6 \pm 0.3$	0(fixed)
CLEO(Fit 2)[26]	$-7.9 \pm 1.9 \pm 0.3$	$1.7 \pm 1.4 \pm 0.3$
Crystal Ball [27]	$-33.3^{+11.6}_{-29.2}$	0(fixed)
E760(Fit 1) [28]	-14 ± 6	0(fixed)
E760(Fit 2) [28]	-14^{+8}_{-7}	0^{+6}_{-5}
E835(Fit 1) [29]	$-9.3^{+3.9}_{-4.1} \pm 0.6$	0(fixed)
E835(Fit 2) [29]	$-7.6^{+5.4}_{-5.0} \pm 0.9$	$2.0^{+5.5}_{-4.4} \pm 0.9$

TABLE III: The M2 and E3 normalized amplitudes $a_2^{J=2}, a_3^{J=2}$ for $\chi_{c2} \rightarrow J/\psi\gamma$ measured by various experiments.

Appendix C: Dilepton angular distribution in χ_c decay with multipole effects

In the appendix, we consider the di-lepton angular distributions of the χ_c which has been discussed in section IX with only E1 transition. Here, we try to include the higher-order multipole effects in $\chi_c \rightarrow J/\psi\gamma \rightarrow \mu^+\mu^-\gamma$. In the section IX, we have discussed two scenarios to describe the angular distributions. Following, we also discuss these two scenarios and generalize the formula to also account for the higher-order multipole contributions.

First, the SDMEs for the J/ψ from the χ_c decay should be generalized as

$$\begin{aligned}
&\rho_{s_z, s'_z}^{\chi_{cJ} \rightarrow J/\psi\gamma} \\
&= \frac{1}{8\pi} \sum_{l=1}^{J+1} \sum_{\lambda_\gamma=\pm l} \int d\Omega [\theta, \phi] \rho_{J_z, J_z}^{\chi_{cJ}} \mathcal{D}_{J_z, J_{1z}}^{J*} \mathcal{D}_{J_z, J_{2z}}^J \\
&\quad \langle l, \lambda_\gamma; 1, s_z | J, J_{1z} \rangle \langle J, J_{2z} | 1, \lambda_\gamma; 1, s'_z \rangle \\
&\quad (2l+1)(a_l^{J=J})^2 \text{Br}(\chi_{cJ} \rightarrow J/\psi\gamma).
\end{aligned} \tag{C1}$$

Hence the coefficients reexpressed as

$$\begin{aligned}
\lambda_{\theta'}^{\chi_{c1}} &= -\frac{1 - 3(a_2^{J=1})^2}{3 - (a_2^{J=1})^2}, \lambda_{\phi'}^{\chi_{c1}} = \lambda_{\phi'}^{\perp\chi_{c1}} = 0, \\
\lambda_{\theta'\phi'}^{\chi_{c1}} &= \frac{\sqrt{2}(a_1^{J=1})^2(\Re(\rho_{1,0}^{\chi_{c1}}) - \Re(\rho_{-1,0}^{\chi_{c1}}))}{4(3 - (a_2^{J=1})^2)N_{\chi_{c1}}}, \\
\lambda_{\theta'\phi'}^{\perp\chi_{c1}} &= -\frac{\sqrt{2}(a_1^{J=1})^2(\Im(\rho_{1,0}^{\chi_{c1}}) + \Im(\rho_{-1,0}^{\chi_{c1}}))}{4(3 - (a_2^{J=1})^2)N_{\chi_{c1}}}, \\
\lambda_{\theta'}^{\chi_{c2}} &= \frac{3(1 - 11(a_2^{J=2})^2 + 9(a_3^{J=2})^2)}{39 + 11(a_2^{J=2})^2 - 9(a_3^{J=2})^2}, \\
\lambda_{\phi'}^{\chi_{c2}} &= \frac{(a_1^{J=2})^2(7\sqrt{6}(\Re\rho_{0,2}^{\chi_{c2}} + \Re\rho_{0,-2}^{\chi_{c2}}) + 12\Re\rho_{1,-1}^{\chi_{c2}})}{2(39 + 11(a_2^{J=2})^2 - 9(a_3^{J=2})^2)N_{\chi_{c2}}}, \\
\lambda_{\theta'\phi'}^{\chi_{c2}} &= [\sqrt{6}(1 - \frac{13}{3}(a_2^{J=2})^2 - (a_3^{J=2})^2)(\Re\rho_{-1,0}^{\chi_{c2}} - \Re\rho_{1,0}^{\chi_{c2}}) \\
&\quad + 6(4 - 9(a_2^{J=2})^2 - 4(a_3^{J=2})^2)(\Re\rho_{-2,-1}^{\chi_{c2}} - \Re\rho_{2,1}^{\chi_{c2}})] \\
&\quad / [4(39 + 11(a_2^{J=2})^2 - 9(a_3^{J=2})^2)N_{\chi_{c2}}], \\
\lambda_{\phi'}^{\perp\chi_{c2}} &= \frac{(a_1^{J=2})^2(7\sqrt{6}(\Im\rho_{0,2}^{\chi_{c2}} - \Im\rho_{0,-2}^{\chi_{c2}}) - 12\Im\rho_{1,-1}^{\chi_{c2}})}{2(39 + 11(a_2^{J=2})^2 - 9(a_3^{J=2})^2)N_{\chi_{c2}}}, \\
\lambda_{\theta'\phi'}^{\perp\chi_{c2}} &= [\sqrt{6}(1 - \frac{13}{3}(a_2^{J=2})^2 - (a_3^{J=2})^2)(\Im\rho_{-1,0}^{\chi_{c2}} + \Im\rho_{1,0}^{\chi_{c2}}) \\
&\quad + 6(4 - 9(a_2^{J=2})^2 - 4(a_3^{J=2})^2)(\Im\rho_{-2,-1}^{\chi_{c2}} + \Im\rho_{2,1}^{\chi_{c2}})] \\
&\quad / [4(39 + 11(a_2^{J=2})^2 - 9(a_3^{J=2})^2)N_{\chi_{c2}}].
\end{aligned} \tag{C2}$$

Again, we find that some polarization observables are trivial and therefore a lot of spin information about the χ_c disappears. However, the observables in the case can be applied to the extraction of multipole amplitudes of χ_c if these observables can be measured sufficiently precise, such as at the electron-positron colliders.

In the second scenario, i.e. the z axis in $J/\psi \rightarrow \mu^+\mu^-$ is chosen to be the same as the quantization axis in the rest frame of the χ_{cJ} , the general relation between the SDMEs of the $\chi_{cJ} \rho_{J_z, J'_z}^{\chi_{cJ}}$ and those of the J/ψ from the χ_{cJ} decay $\rho_{s_z, s'_z}^{\chi_{cJ} \rightarrow J/\psi\gamma}$ with multipole expansion is modified as

$$\begin{aligned}
\rho_{s_z, s'_z}^{\chi_{cJ} \rightarrow J/\psi\gamma} &\propto \sum_{l=1}^{J+1} \sum_{l_z=-l}^l \sum_{J_z, J'_z} (a_l^{J=J})^2 \langle l, l_z; 1, s_z | J, J_z \rangle \\
&\quad \langle J, J'_z | l, l_z; 1, s'_z \rangle \rho_{J_z, J'_z}^{\chi_{cJ}} \text{Br}(\chi_{cJ} \rightarrow J/\psi\gamma).
\end{aligned} \tag{C3}$$

It is clear that the coefficients of the angular distribution

of the μ^+ should be written as

$$\begin{aligned}
\lambda_{\theta'}^{\chi_{c1}} &= \frac{-N_{\chi_{c1}} + 3\rho_{0,0}^{\chi_{c1}}}{R_1}, \\
\lambda_{\phi'}^{\chi_{c1}} &= -\frac{2\Re\rho_{1,-1}^{\chi_{c1}}}{R_1}, \\
\lambda_{\theta'\phi'}^{\chi_{c1}} &= -\frac{\sqrt{2}(\Re\rho_{1,0}^{\chi_{c1}} - \Re\rho_{-1,0}^{\chi_{c1}})}{R_1}, \\
\lambda_{\phi'}^{\perp\chi_{c1}} &= \frac{2\Im\rho_{1,-1}^{\chi_{c1}}}{R_1}, \\
\lambda_{\theta'\phi'}^{\perp\chi_{c1}} &= \frac{\sqrt{2}(\Im\rho_{1,0}^{\chi_{c1}} + \Im\rho_{-1,0}^{\chi_{c1}})}{R_1}, \\
\lambda_{\theta'}^{\chi_{c2}} &= \frac{6N_{\chi_{c2}} - 9(\rho_{1,1}^{\chi_{c2}} + \rho_{-1,-1}^{\chi_{c2}}) - 12\rho_{0,0}^{\chi_{c2}}}{R_2}, \\
\lambda_{\phi'}^{\chi_{c2}} &= \frac{2\sqrt{6}(\Re\rho_{2,0}^{\chi_{c2}} + \Re\rho_{-2,0}^{\chi_{c2}}) + 6\Re\rho_{1,-1}^{\chi_{c2}}}{R_2}, \\
\lambda_{\theta'\phi'}^{\chi_{c2}} &= \frac{6(\Re\rho_{2,1}^{\chi_{c2}} - \Re\rho_{-2,-1}^{\chi_{c2}}) + \sqrt{6}(\Re\rho_{1,0}^{\chi_{c2}} - \Re\rho_{-1,0}^{\chi_{c2}})}{R_2}, \\
\lambda_{\phi'}^{\perp\chi_{c2}} &= \frac{2\sqrt{6}(\Im\rho_{0,2}^{\chi_{c2}} - \Im\rho_{0,-2}^{\chi_{c2}}) - 6\Im\rho_{1,-1}^{\chi_{c2}}}{R_2}, \\
\lambda_{\theta'\phi'}^{\perp\chi_{c2}} &= \frac{6(\Im\rho_{1,2}^{\chi_{c2}} + \Im\rho_{-1,-2}^{\chi_{c2}}) + \sqrt{6}(\Im\rho_{0,1}^{\chi_{c2}} + \Im\rho_{0,-1}^{\chi_{c2}})}{R_2},
\end{aligned} \tag{C4}$$

with

$$\begin{aligned}
R_1 &= [(15 - 2(a_2^{J=1})^2)N_{\chi_{c1}} \\
&\quad - (5 - 6(a_2^{J=1})^2)\rho_{0,0}^{\chi_{c1}}]/(5 - 6(a_2^{J=1})^2), \\
R_2 &= [2(21 + 14(a_2^{J=2})^2 + 5(a_3^{J=2})^2)N_{\chi_{c2}} \\
&\quad + 3(7 - 14(a_2^{J=2})^2 - 5(a_3^{J=2})^2)(\rho_{1,1}^{\chi_{c2}} + \rho_{-1,-1}^{\chi_{c2}}) \\
&\quad + 4(7 - 14(a_2^{J=2})^2 - 5(a_3^{J=2})^2)\rho_{0,0}^{\chi_{c2}}] \\
&\quad / (7 - 14(a_2^{J=2})^2 - 5(a_3^{J=2})^2).
\end{aligned}$$

Similarly, the feed-down contributions should be modified to account for the complete multipole effects.

-
- [1] N. Brambilla, S. Eidelman, B. Heltsley, R. Vogt, G. Bodwin, *et al.*, “Heavy quarkonium: progress, puzzles, and opportunities,” *Eur.Phys.J.* **C71** (2011) 1534, 1010.5827. For a very recent review of heavy quarkonium production, see also G. Bodwin, arXiv:1208.5506.
- [2] G. T. Bodwin, E. Braaten, and G. Lepage, “Rigorous QCD analysis of inclusive annihilation and production of heavy quarkonium,” *Phys.Rev.* **D51** (1995) 1125–1171, hep-ph/9407339.
- [3] E. Braaten, B. A. Kniehl, and J. Lee, “Polarization of prompt J/ψ at the Tevatron,” *Phys.Rev.* **D62** (2000) 094005, hep-ph/9911436.
- [4] **CDF Collaboration**, T. Affolder *et al.*, “Measurement of J/ψ and $\psi(2S)$ polarization in $p\bar{p}$ collisions at $\sqrt{s} = 1.8$ TeV,” *Phys.Rev.Lett.* **85** (2000) 2886–2891, hep-ex/0004027.
- [5] **CDF Collaboration**, A. Abulencia *et al.*, “Polarization of J/ψ and ψ_{2S} mesons produced in $p\bar{p}$ collisions at $\sqrt{s} = 1.96$ -TeV,” *Phys.Rev.Lett.* **99** (2007) 132001, 0704.0638.
- [6] P. Faccioli, C. Lourenco, J. Seixas, and H. K. Wohri, “Towards the experimental clarification of quarkonium polarization,” *Eur.Phys.J.* **C69** (2010) 657–673, 1006.2738.
- [7] **CDF Collaboration**, A. Abulencia *et al.*, “Measurement of $\sigma_{\chi_{c2}}\mathcal{B}(\chi_{c2} \rightarrow J/\psi\gamma)/\sigma_{\chi_{c1}}\mathcal{B}(\chi_{c1} \rightarrow J/\psi\gamma)$ in $p\bar{p}$ collisions at $\sqrt{s} = 1.96$ -TeV,” *Phys.Rev.Lett.* **98** (2007) 232001, hep-ex/0703028.
- [8] Y.-Q. Ma, K. Wang, and K.-T. Chao, “QCD radiative corrections to χ_{cJ} production at hadron colliders,” *Phys.Rev.* **D83** (2011) 111503, 1002.3987.
- [9] **LHCb Collaboration**, R. Aaij *et al.*, “Measurement of the cross-section ratio $\sigma(\chi_{c2})/\sigma(\chi_{c1})$ for prompt χ_c production at $\sqrt{s} = 7$ TeV,” 1202.1080.
- [10] J. M. Campbell, F. Maltoni, and F. Tramontano, “QCD corrections to J/ψ and Upsilon production at hadron colliders,” *Phys.Rev.Lett.* **98** (2007) 252002, hep-ph/0703113.
- [11] B. Gong, X. Q. Li, and J.-X. Wang, “QCD corrections to J/ψ production via color octet states at Tevatron and LHC,” *Phys.Lett.* **B673** (2009) 197–200, 0805.4751.
- [12] M. Butenschoen and B. A. Kniehl, “Reconciling J/ψ production at HERA, RHIC, Tevatron, and LHC with NRQCD factorization at next-to-leading order,” *Phys.Rev.Lett.* **106** (2011) 022003, 1009.5662.
- [13] Y.-Q. Ma, K. Wang, and K.-T. Chao, “ J/ψ (ψ') production at the Tevatron and LHC at $O(\alpha_s^4 v^4)$ in nonrelativistic QCD,” *Phys.Rev.Lett.* **106** (2011) 042002, 1009.3655.
- [14] Y.-Q. Ma, K. Wang, and K.-T. Chao, “A complete NLO calculation of the J/ψ and ψ' production at hadron colliders,” *Phys.Rev.* **D84** (2011) 114001, 1012.1030.
- [15] B. Gong and J.-X. Wang, “Next-to-leading-order QCD corrections to J/ψ polarization at Tevatron and Large-Hadron-Collider energies,” *Phys.Rev.Lett.* **100** (2008) 232001, 0802.3727.
- [16] Z.-B. Kang, J.-W. Qiu, and G. Sterman, “Heavy quarkonium production and polarization,” *Phys.Rev.Lett.* **108** (2012) 102002, 1109.1520. latex, 11 pages, 4 figures.

- [17] P. Artoisenet, J. M. Campbell, J. Lansberg, F. Maltoni, and F. Tramontano, “ Υ Production at Fermilab Tevatron and LHC Energies,” *Phys.Rev.Lett.* **101** (2008) 152001, 0806.3282.
- [18] M. Butenschoen and B. A. Kniehl, “J/psi polarization at Tevatron and LHC: Nonrelativistic-QCD factorization at the crossroads,” *Phys. Rev. Lett* **108** (2012) 172002, 1201.1872.
- [19] K.-T. Chao, Y.-Q. Ma, H.-S. Shao, K. Wang, and Y.-J. Zhang, “ J/ψ polarization at hadron colliders in nonrelativistic QCD,” *Phys. Rev. Lett* **108** (2012) 242004, 1201.2675.
- [20] **ATLAS Collaboration**, G. Aad *et al.*, “Measurement of the differential cross-sections of inclusive, prompt and non-prompt J/psi production in proton-proton collisions at $\sqrt{s} = 7$ TeV,” *Nucl. Phys.* **B850** (2011) 387–444, 1104.3038.
- [21] **CMS Collaboration**, S. Chatrchyan *et al.*, “J/psi and psi(2S) production in pp collisions at $\sqrt{s} = 7$ TeV,” *JHEP* **02** (2012) 011, 1111.1557.
- [22] M. Butenschoen and B. A. Kniehl, “World data of J/psi production consolidate NRQCD factorization at NLO,” *Phys.Rev.* **D84** (2011) 051501, 1105.0820.
- [23] B. A. Kniehl, G. Kramer, and C. P. Palisoc, “chi(c1) and chi(c2) decay angular distributions at the Fermilab Tevatron,” *Phys.Rev.* **D68** (2003) 114002, hep-ph/0307386.
- [24] P. Faccioli, C. Lourenco, J. Seixas, and H. K. Wohri, “Determination of χ_c and χ_b polarizations from dilepton angular distributions in radiative decays,” *Phys.Rev.* **D83** (2011) 096001, [arXiv:1103.4882].
- [25] M. Beneke, M. Kramer, and M. Vanttinen, “Inelastic photoproduction of polarized J / psi,” *Phys.Rev.* **D57** (1998) 4258–4274, hep-ph/9709376.
- [26] **CLEO Collaboration**, M. Artuso *et al.*, “Higher-order multipole amplitudes in charmonium radiative transitions,” *Phys.Rev.* **D80** (2009) 112003, 0910.0046.
- [27] **Crystal Ball Collaboration**, M. Oreglia *et al.*, “Study of the reaction $\psi' \rightarrow \gamma\gamma J/\psi$,” *Phys.Rev.* **D25** (1982) 2259.
- [28] **E760 Collaboration**, T. A. Armstrong *et al.*, “Study of the angular distribution of the reaction $\bar{p}p \rightarrow \chi_{c2} \rightarrow J/\psi\gamma \rightarrow e^+e^-\gamma$,” *Phys.Rev.* **D48** (1993) 3037.
- [29] **E835 Collaboration**, M. Ambrogiani *et al.*, “Study of the angular distributions of the reactions $\bar{p}p \rightarrow \chi_{c1}, \chi_{c2} \rightarrow J/\psi\gamma \rightarrow e^+e^-\gamma$,” *Phys.Rev.* **D65** (2002) 052002.
- [30] C. S. Lam and W. -K. Tung, “A Systematic Approach To Inclusive Lepton Pair Production In Hadronic Collisions,” *Phys. Rev.* **D18** (1978) 2447.
- [31] C. S. Lam and W. -K. Tung, “A Parton Model Relation Sans Qcd Modifications In Lepton Pair Productions,” *Phys.Rev.* **D21** (1980) 2712 .
- [32] E. L. Berger, J. -W. Qiu and R. A. Rodriguez-Pedraza, “Transverse momentum dependence of the angular distribution of the Drell-Yan process,” *Phys.Rev.* **D76** (2007) 074006, [arXiv:0708.0578 [hep-ph]].
- [33] P. Faccioli, C. Lourenco and J. Seixas, “Rotation-invariant relations in vector meson decays into fermion pairs,” *Phys. Rev. Lett.* **105** (2010) 061601 , [arXiv:1005.2601 [hep-ph]].
- [34] B. A. Kniehl and J. Lee, “Polarized J/ψ from chi(cJ) and ψ' decays at the Tevatron,” *Phys.Rev.* **D62** (2000) 114027, hep-ph/0007292.
- [35] S. Chung and T. Trueman, “Positivity Conditions on the Spin Density Matrix: A Simple Parametrization,” *Phys.Rev.* **D11** (1975) 633.
- [36] E. J. Eichten and C. Quigg, “Quarkonium wave functions at the origin,” *Phys.Rev.* **D52** (1995) 1726–1728, hep-ph/9503356.
- [37] A. Kanaki and C. G. Papadopoulos, “HELAC: A package to compute electroweak helicity amplitudes,” *Comput. Phys. Commun.* **132** (2000) 306–315, hep-ph/0002082.
- [38] C. Papadopoulos and M. Worek, “HELAC - A Monte Carlo generator for multi-jet processes,” hep-ph/0606320.
- [39] C. G. Papadopoulos, “PHEGAS: A phase space generator for automatic cross- section computation,” *Comput. Phys. Commun.* **137** (2001) 247–254, hep-ph/0007335.
- [40] A. Cafarella, C. G. Papadopoulos, and M. Worek, “Helac-Phegas: a generator for all parton level processes,” *Comput. Phys. Commun.* **180** (2009) 1941–1955, 0710.2427.
- [41] R. Kleiss, W. Stirling, and S. Ellis, “A NEW MONTE CARLO TREATMENT OF MULTIPARTICLE PHASE SPACE AT HIGH-ENERGIES,” *Comput.Phys.Commun.* **40** (1986) 359.
- [42] G. Lepage, “A New Algorithm for Adaptive Multidimensional Integration,” *J.Comput.Phys.* **27** (1978) 192. Revised version.
- [43] J. Pumplin, D. Stump, J. Huston, H. Lai, P. M. Nadolsky, *et al.*, “New generation of parton distributions with uncertainties from global QCD analysis,” *JHEP* **0207** (2002) 012, hep-ph/0201195.
- [44] E. Braaten and T. C. Yuan, “Gluon fragmentation into P wave heavy quarkonium,” *Phys.Rev.* **D50** (1994) 3176–3180, hep-ph/9403401.
- [45] E. Braaten, D. Kang, J. Lee, and C. Yu, “Optimal spin-quantization axes for quarkonium with large transverse momentum,” *Phys.Rev.* **D79** (2009) 054013, [arXiv:0812.3727].
- [46] B. Gong, L.-P. Wan, J.-X. Wang, H.-F. Zhang, “Polarization for Prompt $J/\psi(\psi')$ production at the Tevatron and LHC,” , 1205.6682.